FORAMINIFERA, TIDAL NOTCHES, & NEOTECTONIC EVENTS IN GREECE

FORAMINIFERA AND TIDAL NOTCHES: DATING NEOTECTONIC EVENTS AT KORPHOS, GREECE

Chantel F. Nixon

A Thesis

Submitted to the School of Graduate Studies

in partial fulfillment of the requirements

for the Degree Master of Science

McMaster University, Hamilton, Ontario

MASTER OF SCIENCE (2001) McMASTER UNIVERSITY
School of Geography and Geology Hamilton, Ontario

TITLE: Foraminifera and tidal notches: dating neotectonic events at Korphos, Greece

AUTHOR: Chantel F. Nixon, B.Sc. (McMaster University)

SUPERVISOR: Dr. E.G. Reinhardt

NUMBER OF PAGES: ix, 116

ABSTRACT

Foraminiferal and thecamoebian biofacies were documented in the modern Korphos marsh located on the western coast of the Saronikos Gulf, Greece in order to define the general ecological features (such as salinity and proximity to marine influence) of the environments they occupied. These constraints were later used to identify fossil biofacies in subsurface marsh sediments at Korphos.

Positive marine tendencies identified in fossil biofacies distributions were used for the first time to radiocarbon date relative changes in sea-level implied by a series of discrete, submerged tidal notches and beach rock adjacent to the marsh along the coast. Magnitude of subsidence events based on notch and beach rock data were measured to 2.9m, 0.5m, 1.3m, 0.39m, 0.47m, and 0.34m. The relatively unaltered v-shape of each notch profile suggested that sea-level rise was rapid and episodic.

A comparison between the tidal notches and beach rock and an isostatically-corrected model of sea-level for this area isolated the tectonic contribution to sea-level change and revealed that at least four of the six sea-level indicators plotted well-below predicted sea-level during subsidence. Therefore, the gradual sea-level rise of the late Holocene was interrupted by at least four sub-meter to meter-scale, step-wise increases in relative sea-level during coseismic subsidence of the Korphos marsh. The results of this study show how the combination of geomorphological and salt-marsh records have the potential to remove errors stemming from a lack of datable material for notches and autocompaction of marsh sediments when reconstructing local sea-level change.

ACKNOWLEDGMENTS

My biggest thanks go to Dr. Eduard Reinhardt, my supervisor and friend, for the opportunities and guidance he has given me over the past two years. I am so grateful for the skills I have developed under his supervision and feel they will allow me to confidently pursue my next exciting challenge in the world of foraminifera. I will never forget SCUBA diving in the Mediterranean, nor my days as a graduate student under his supervision at McMaster University.

Many thanks are also extended to Richard Rothaus at St. Cloud State University, who started this project, patiently answered my questions, and generously sent maps and other important data my way, right up until the end. Thanks to Fleur Leslie for her assistance in the lab.

My sincerest gratitude is extended to Patty Meyer (pants), my best pal, for her kindness and generosity, but mostly for the person she is and the fun we had. Special thanks to Mark Taylor for the support, comfort, and advice he provided over this last year in particular. Even though far away, he was always the light at the end of the tunnel and kept me working through the frustration.

To all of my micropalaeo-lab-mates, Krista, Beverly, Jenny, and Laura: thank you all for your support, interest, and patience while I wrote, revised, revised, revised, and re-wrote my thesis. Thanks to Jim, Bev, and Nili for sharing their new home with me over the last two months and for forcing me out of the office when I was over-tired and hungry! Thanks also to Mike, Emmanuelle, Feride, Owen, Heather, Sarah and Dr. Jack Rink, for the inspiration and much-needed distraction from school.

Finally, I would like to dedicate this thesis to my family: Mom, Dad, Brent, and Jaimie. Each and every one of them, in their own unique way, managed to motivate and support me during their own troubled times. The generosity and love extended has been overwhelming, and I could never have completed this degree without them.

TABLES OF CONTENTS

LIST OF FIGURES

LIST OF TABLES

CHAPTER 1: INTRODUCTION

Abundant surficial geomorphological evidence for Holocene sea-level change can be found in the form of raised or submerged coastal landforms such as beach ridges, caves, reefs, and notches. By mapping and recording elevations of these features, the positions of former coastlines can be established and the vertical range of sea-level variations estimated. In many situations however, a complete picture of sea-level change can only be obtained by combining geomorphological data with evidence from the stratigraphic record. Salt-marsh deposits form a relatively continuous record of sea-level change compared with the often fragmentary geomorphological evidence, and many littoral sedimentary sequences contain fossils which provide additional data for the reconstruction of sea-level histories. Furthermore, sedimentological and biological evidence allows dating and correlation of sea-level variations, whereas geomorphological evidence is more difficult to date precisely. However, autocompaction during sediment accretion can alter the original elevation of marsh deposits and decompaction models are difficult to develop. By combining coastal landform data with sedimentary and fossil records from core data, problems encountered with notch dates and autocompaction of marsh sediments are minimized and a sequence of sea-level changes in a particular locality can be established (Smith and Dawson, 1983; Devoy, 1987; Tooley and Shennan, 1987).

Sea-level change can also be recognized by various archaeological indicators, the most useful of which imply specific activities related to the waterfront such as harbor structures, piscinas, and coastal wells (Pirazzoli, 1996; Sivan et al, 2001). Ages of archaeological indicators are more easily obtained than they are for geomorphological

indicators but precise elevation with respect to sea-level is not always clear. Furthermore, the nature of relative sea-level change, whether it was gradual due to eustatic or isostatic factors or rapid due to an earthquake, cannot usually be determined from the archaeological record alone.

Korphos marsh, located in the region of Korinthia along the northwestern shoreline of the Saronikos Gulf, Greece is an ideal site for sea-level reconstruction (Fig. 1, Chapter 2) as salt marshes respond quickly to even minor changes in sea-level (Cundy, et al., 2000). Evidence for sea-level change in the area is particularly obvious at archaeological sites, especially harbors, scattered along the Korinthian coastline. Lechaion harbor, situated along the Korinthiakos Gulf for example, is currently above sea-level, while the ancient harbor of Kenchreai along the Saronikos Gulf is submerged. These harbors are oft-cited examples of tectonic disruption of important trade routes in ancient Greece (Noller et al., 1997). Korphos, a lesser-known harbor of the Korinthia along the Saronikos Gulf, was likely also subject to multiple incidents of seismic activity and relative sea-level change.

The existence of five, laterally continuous, submerged wave-cut notches immediately south of Korphos marsh indicate that coseismic subsidence indeed took place here, probably due to fault motion (Fig. 2, Chapter 3). However, notch evidence alone may lead to ambiguous interpretations since the effects of an instantaneous movement cannot always be distinguished from the effects of events lasting for decades or even for a few centuries and dating submerged notches is very difficult. To be fully convincing, the interpretation of a movement as coseismic should include a cluster of

converging indicators, suggesting that the displacement could have taken place only in a very brief space of time.

This study will attempt for the first time to correlate and radiocarbon date marine notches (which do not suffer from compaction) with adjacent marsh stratigraphy and the foraminiferal record. The relative sea-level record will them be compared to an isostatically modeled sea-level curve of the area to determine and date neotectonic events. This information will provide a relative sea-level history for the local area to predict older shorelines and the links with the archaeological record in the Korinthia.

The thesis is organized in the following manner. Chapter 2 is a detailed study of modern marsh foraminiferal distributions, documenting the general environmental settings and proximities to sea-level of modern foraminiferal assemblages in Korphos marsh. In Chapter 3, stratigraphy, microfossil, and radiometric (^{14}C) data from Korphos marsh sediment cores and their correlation with marine notches were used to determine a relative sea-level history for the area. This record was then compared with an isostatic model of sea-level change to estimate the timing and magnitude of neotectonic activity for the Korphos area.

CHAPTER 2: FORAMINIFERAL DISTRIBUTION IN THE MODERN KORPHOS MARSH

2.0 ABSTRACT

Three foraminiferal biofacies from a microtidal salt marsh on the northeastern shore of the Saronikos Gulf, Greece, were identified through cluster analysis. Low-Marsh I, Low-Marsh II, and Upper-High-Marsh labels were assigned to assemblages dominated by *Milliammina fusca*, *Trochammina inflata/Trochammina macrescens*, and *Centropyxis aculeata* respectively. Due to a cobble beach barrier, only occasional flooding of the marsh surface occurs, thus preventing a regular salinity gradient related to tidal range and marsh elevation from establishing itself. Rather, the dominant controls on marsh salinity and foraminiferal distributions were interpreted to be microtopography, climate, seepage from freshwater springs, and seawater influx through a drainage ditch that runs along the southern edge of the marsh. Consequently, foraminiferal zonations do not follow as clear an elevational trend as has been found in other marshes. The Upper-High Marsh biofacies of this study consists almost exclusively of thecamoebians with minor amounts of *T. macrescens*, and is at the highest elevation in the marsh and the furthest away from marine influence. The low marsh is very heterogeneous in faunal composition and was divided into two subfacies: Low-Marsh I and Low-Marsh II. The Low-Marsh I biofacies was found between -0.06m and 0.14m, and was dominated by *M. fusca*. The Low-Marsh II biofacies on the other hand, occupied a lower vertical zone within the marsh between -0.29m and 0.05m and consisted mainly of trochamminids with a smaller *M. fusca* component.

2.1 INTRODUCTION TO THE MODERN MARSH SURVEY

Detailed descriptions of foraminiferal zonations have been reported for salt marshes around the world, including Atlantic and Pacific North America, Chile, Greece, New Zealand, and Japan (Scott et al., 1979; Patterson, 1990; Jennings and Nelson, 1992; Gehrels, 1994; Jennings et al., 1995; Nelson et al., 1996; Scott et al., 1996; Hayward et al., 1999; Williams, 1999). These studies show that although species composition of zones varies between areas with differing salinity, substrate, tidal range, and climate, vertical extent of the zones is similar, especially in the high marsh. Such zones are useful for interpreting and locating former sea-levels through the use of marsh sediment cores. This study tests this trend in a different marsh setting; one that does not receive regular tidal inundations due to a cobble beach barrier.

2.1.1 Marsh Physiography

Korphos Bay, located along the northwestern coastline of the Saronikos Gulf, Greece, contains a previously unstudied microtidal-range (<0.30m) salt marsh (Fig. 1). Marsh elevations here range from approximately 0.25m below MSL (mean sea-level) to 0.30m above MSL. Total relief is therefore less than 1.0m from beach barrier to landward margins (Fig. 2).

Limestone hills in the area rise close to the shoreline and the drop off on the continental slope is steep. Three NW-SE faults, one cutting the western corner of the marsh, and two running parallel and south of the first, have freshwater springs that flow into the marsh and also offshore and along the coast. Freshwater seepage from these

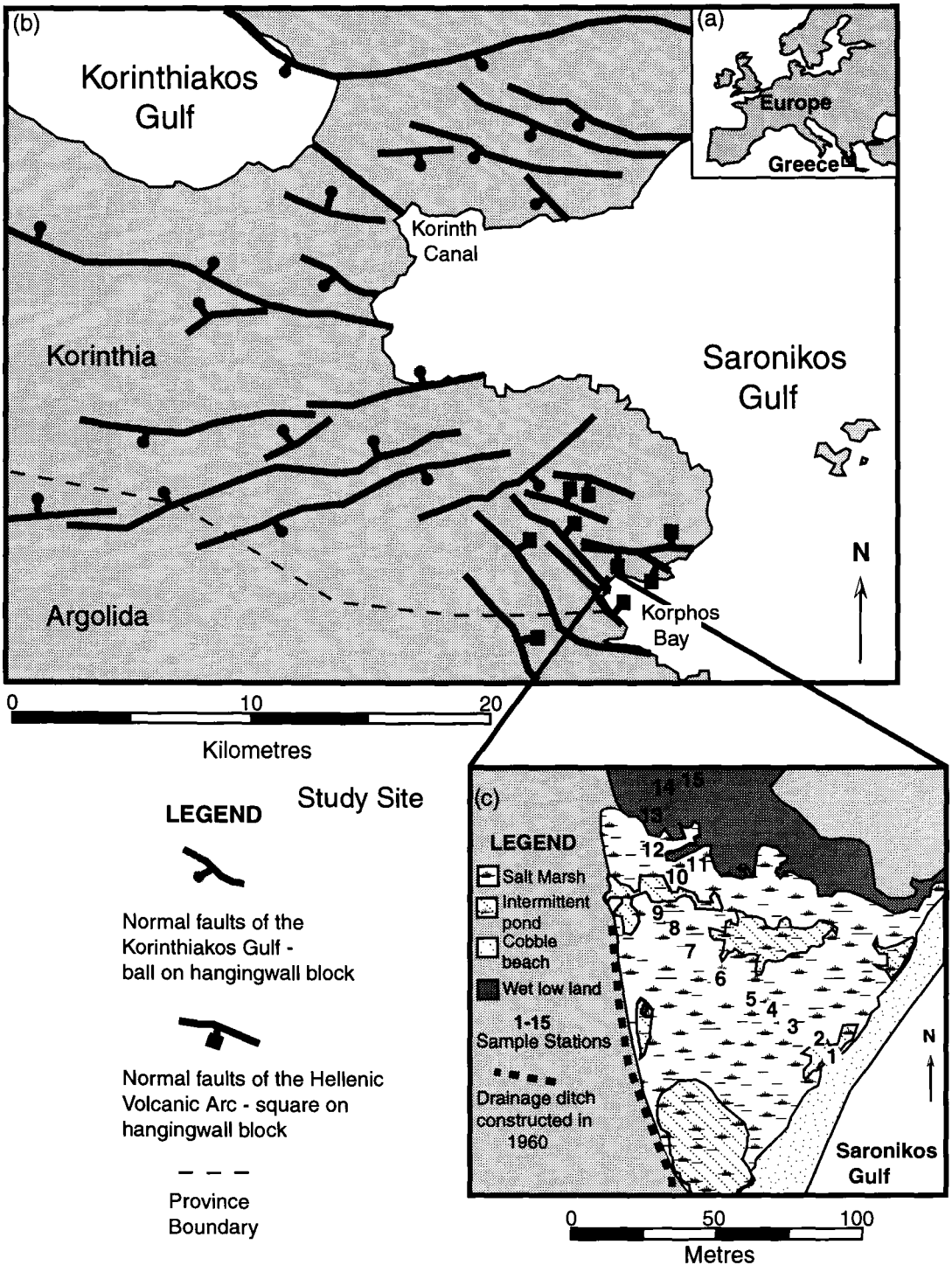

Figure 2.1: (a) Location of Greece in Europe. (b) Southeastern corner of the province of Korinthia where Korphos Bay is located. (c) Salt marsh (study site) in Korphos Bay.

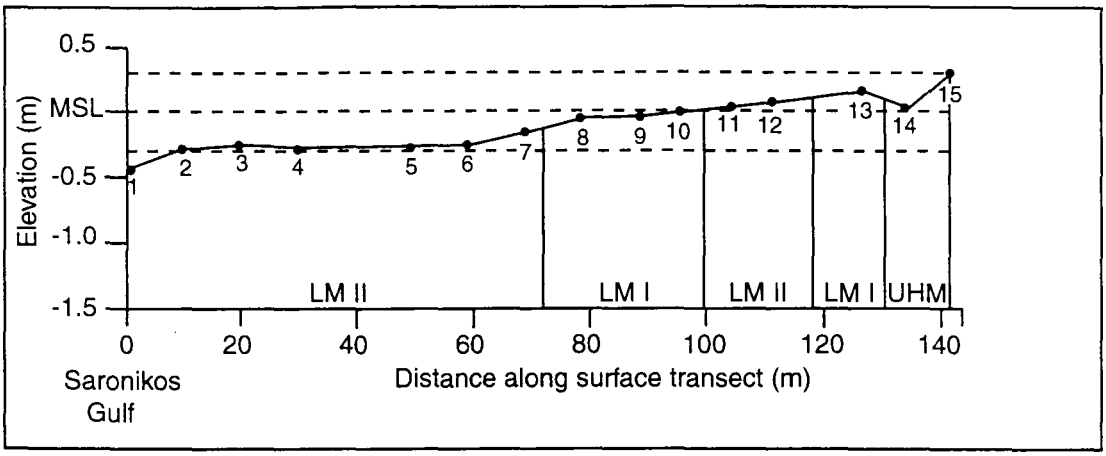

Figure 2.2: Surface Transect of Korphos Marsh with Biofacies labelled.
LM II = Low Marsh II biofacies; LM I = Low Marsh biofacies; UHM = Upper-High-Marsh biofacies. ⋮⋮⋮ = upper and lower tidal limits. Middle bar indicates MSL.

springs creates unusual salinity gradients within the marsh environment. Salinity values recorded in June, 1998 along the transect were consistently less than 30 parts per thousand (14-27 ppt), which is lower than expected considering the high rates of evaporation and low precipitation of the Greek climate during the summer season (Table 1). These values are similar to those reported by Scott et al. (1979) for marshes along the northwest side of the Gulf of Patras, Greece, during the wetter, winter month of December (12-27 ppt). This comparison reveals the importance of spring water seepage to surface salinity.

Korphos marsh is also atypical in that it is closed to the Saronikos Gulf by a cobble beach barrier (approximately 0.5m above MSL) that prevents flooding of the marsh except during winter storms. Attempts to drain the marsh and minimize outbreaks of malaria in 1950-60 were made via construction of a drainage ditch (approximately 0.75m wide) along the southern edge of the marsh running perpendicular to the coastline (Fig. 1). The ditch created a pathway for seawater from the Saronikos Gulf to enter the marsh during storms and seiches, and to some extent during high tide. Studies of foraminiferal zonation in semi-closed marsh systems such as the one at Korphos are few (Alve and Murray, 1995, 1999), and highlight the significance of this particular study.

The location of Korphos marsh in tectonically active central Greece also makes it ideal for identifying late Quaternary and Holocene sea-level changes in older, littoral sediments. This study will define the surface distributions of foraminifera at Korphos for their later use in the examination of long cores taken from the marsh. The results from

Sample number		2	3	4	5	6	7	8	9	10	11	12	13	14	15
Elevation (m above or below MSL)		-0.29	-0.26	-0.29	-0.28	-0.27	-0.17	-0.06	-0.05	NA	NA	0.05	0.14	0.02	0.29
Salinity (ppt)		18	18	18	14	20	20	20	20	20	20	20	20	18	27
Biofacies		LM II	LM II	LM II	LM II	LM II	LM II	LM I	LM I	LM I	LM II	LM II	LM I	UHM	UHM
Total Counts		800	679	536	537	369	475	394	88	92	479	460	263	55	340
Specimens per 1 cc		320	506	1876	3373	1104	2797	290	19	12	508	412	479	22	136
Ammonia beccarii "tepida"	L/T	100	-	-	-	-	-	-	-	-	-	50	-	-	-
	T	×	-	-	-	-	-	-	-	-	-	×	×	-	-
Arcella vulgaris	L/T	-	7	-	-	-	-	-	-	-	-	-	-	-	-
	T	×	4	1	×	×	×	9	×	×	×	×	3	×	×
Centropyxis aculeata	L/T	-	100	-	-	-	-	-	-	-	-	-	-	-	-
	T	×	×	×	×	×	2	2	×	×	9	×	11	71	83
Centropyxis constricta	L/T	-	-	-	-	-	50	-	-	-	-	-	-	-	-
	T	-	2	4	-	-	×	18	-	-	-	×	1	-	15
Discorynopsis aquayoi	L/T	40	100	100	-	-	-	13	-	-	-	57	53	-	-
	T	×	×	×	-	-	-	2	-	-	6	×	2	16	-
Miliammina fusca	L/T	12	4	5	2	8	12	5	-	-	-	-	-	-	-
	T	3	38	23	8	4	10	49	58	50	11	4	80	-	-
Trochammina inflata	L/T	13	8	18	4	20	22	14	-	33	22	×	40	-	-
	T	67	48	51	49	64	52	15	4	10	37	51	×	-	-
Trochammina macrescens	L/T	20	14	8.	4	13	14	12	6	42	5	11	23	-	-
	T	29	7	21	43	32	36	6	38	40	37	44	3	13	1

Table 2.1: Foraminifera and thecamoebian data in relative frequency form, calculated from specimens per 1 cc. × = < 1%; L/T = percent of total that was alive at the time of collection; MSL = mean sea-level; LM II = Low Marsh II biofacies; LM I = Low Marsh I biofacies; UHM = Upper-High-Marsh biofacies.

this study are critical for interpreting the microfossil record and reconstructing rates of local sea-level change in this area for the past 5000 years.

2.1.2 Taphonomic and Seasonal Considerations

Taphonomic and seasonal changes affecting surficial foraminiferal distributions need to be considered before using such assemblages to interpret foraminiferal zonations in the fossil record. Modern intertidal and subtidal foraminiferal populations of the Samish Bay salt marshes, located along the Pacific coast of Washington, U.S.A. for example, differed in the spring and summer months from the fall and winter due to seasonal reproduction in the spring and early fall (Jones and Ross, 1979). However, in a comparison of Greek and southern California salt marsh foraminifera, Scott et al. (1979) found no evidence of seasonal change in either of the assemblages and attributed this to minimal annual temperature fluctuations. Differential preservation of foraminifera may also vary according to latitude and therefore climate, due to differences in metabolizability of organic matter (Reaves, 1986; Hippensteel et al., 2000).

In order to remove any effects of seasonal overprinting for palaeoenvironmental reconstruction, Horton (1999) found that death assemblages from the surface most accurately reflect that which is preserved in the subsurface (Horton, 1999). Murray (1971, 2000) argued strongly against the use of either death or total assemblages in ecological studies however, stating that the death assemblage component of the total is taphonomically altered and thus an artefact. Such alteration frequently manifests itself in fragile, low marsh foraminiferal populations. Species such as agglutinated *Milliaminna*

fusca, and calcareous *Ammonia beccarii* can be lost via oxidation of the organic test cements and via dissolution respectively (Martin, 1999). *M. fusca* may be susceptible to degradation by oxidation in the top 10 cm of sediment (Goldstein and Watkins, 1998). If taphonomic alteration occurs, fossil assemblages may be dominated by the more robust, high marsh species that originally comprised much smaller proportions of the living assemblage (Goldstein et al., 1995). Nevertheless, the majority of researchers studying salt marsh foraminiferal zonation have relied on total populations because they feel they most accurately represent the general environmental conditions, integrating both seasonal and temporal fluctuations (Buzas, 1968; Scott and Leckie, 1990; Patterson, 1990; Williams, 1994; Jennings et al., 1995; Ozarko et al., 1997).

In light of the considerations discussed above, rather than using a global model for salt marsh foraminifera and elevation above MSL (Scott and Medioli, 1980), it seems imperative that the unique opportunistic behavior of modern Korphos foraminifera is documented in as much detail as possible to evaluate their potential as palaeoenvironmental indicators.

2.2. METHODS

Samples of marsh sediments were collected at a regular interval from 14 sample sites along a 140 m transect running normal to the coastline (Fig. 2). The sampling strategy aimed to cover all areas which could serve as modern equivalents of former ecological situations. Traditional work on surface distributions of salt-marsh foraminifera has relied on sampling the top 1 cm of sediment, but in a review by Ozarko et al. (1997) and Goldstein and Watkins (1998), an assessment of the top 10 cm was found to provide a more accurate representation of the modern assemblage. Taking this into consideration, 10 cm deep samples were collected from the Korphos marsh. Sample elevations were measured using a level in relation to the modern solution notch cut into limestone cliffs along the shoreline in the southern end of the embayment at Korphos. Salinity was recorded at each sample station using an optical salinity refractometer (Table 1). This device is convenient for measuring interstitial water in drier marsh areas (Scott and Medioli, 1980).

In the lab 10 cc samples were washed through a 63 μm sieve and later dyed with Rose Bengal stain to determine those specimens that were alive at the time of collection. All samples were examined wet to facilitate the appearance of the Rose Bengal dye and to prevent degradation of the agglutinated fauna.

Foraminiferal identification and counts were performed using a binocular dissecting microscope (60 to 95 × magnification) and photographs of each species were taken using an Environmental Scanning Electron Microscope 2020 (Biology Department, McMaster University; Plate 1, Appendix A).

In order to statistically determine biofacies and marsh zones, a count of at least 300 specimens was considered representative (Patterson et al. 1989). If a sample had very high abundances, it was split into equal portions and one or more subsamples sufficed for the counting (Scott, 1999). Of the 14 samples analyzed, a total of 8 statistically significant thecamoebian and foraminiferal species were found. To gauge the uncertainty on species abundance, Patterson and Fishbein's (1989) methods for determining uncertainty were adopted with the standard error calculated using the following equation (Appendix B):

$$SX_i = [X_i(1 - X_i)/N]^{1/2}$$

SX_i is the standard error; X_i is the estimated fractional abundance for each i = 1, 2, 3, ..., I species; where I = the total number of species in a particular sample; i is each species; and N is the total number of specimens counted in a sample. When making N counts, the actual fractional abundance f_i lies between,

$$X_i - 1.96\ SX_i \leq f_i \leq X_i + 1.96\ SX_i$$

95% of the time regardless of the number of the species contained in the sample. The 95% confidence interval on the estimated fractional abundances is therefore,

$$X \pm 1.96\ SX_i$$

Q-mode cluster analysis was performed on the data set using the statistical package SAS JMP v. 3 on a Power Macintosh (7300/180) personal computer. The resulting hierarchical dendogram divided the samples into disjoint sets and was used to determine the various biofacies present within the modern Korphos marsh. The best results according to Fishbein and Patterson's (1993) Error Weighted Maximum

Likelihood (EWML) clustering method are obtained by first reducing the data set by removing the rare species. The data set from Korphos was reduced by removing the rare species *Ammonia beccarii "tepida"* that was consistently less than 1% abundant and only observed in three samples (Table 1).

2.3. BIOFACIES

Cluster analysis of foraminiferal abundance in each of the 14 surface samples revealed three distinct clusters that, based on their dominant faunal assemblages (Fig. 3) and previously-documented ecological constraints, could be divided into Low-Marsh I, Low-Marsh II, and Upper-High-Marsh biofacies (Fig. 4).

2.3.1. Low-Marsh I biofacies

In Samples 8-10 and 13 which make up the Low-Marsh I biofacies, *M. fusca*, the common low marsh indicator species, had a mean relative abundance of 47% ± 34 (Table 2). The highest relative abundance of *M. fusca* (80%) was observed in sample 13, located approximately 100m from the Saronikos Gulf.

Normally, *M. fusca* occupy environments where regular tidal flooding of the marsh occurs (Scott and Medioli, 1978; Patterson, 1990; Scott and Leckie, 1990; Jennings and Nelson, 1992; Gehrels, 1994; Horton, 1999) and are thus good indicators of mean high and low tidal ranges. Marine flooding of Korphos marsh however is not frequent enough to stabilize and homogenize salinity gradients and therefore create distinct high and low marsh zones related to a specific elevation above MSL. *M. fusca* was able to dominate certain regions of the Korphos marsh due to unusual salinity gradients created by evaporation and the artificial drainage channel, which represents the only pathway for seawater from the gulf to enter the marsh.

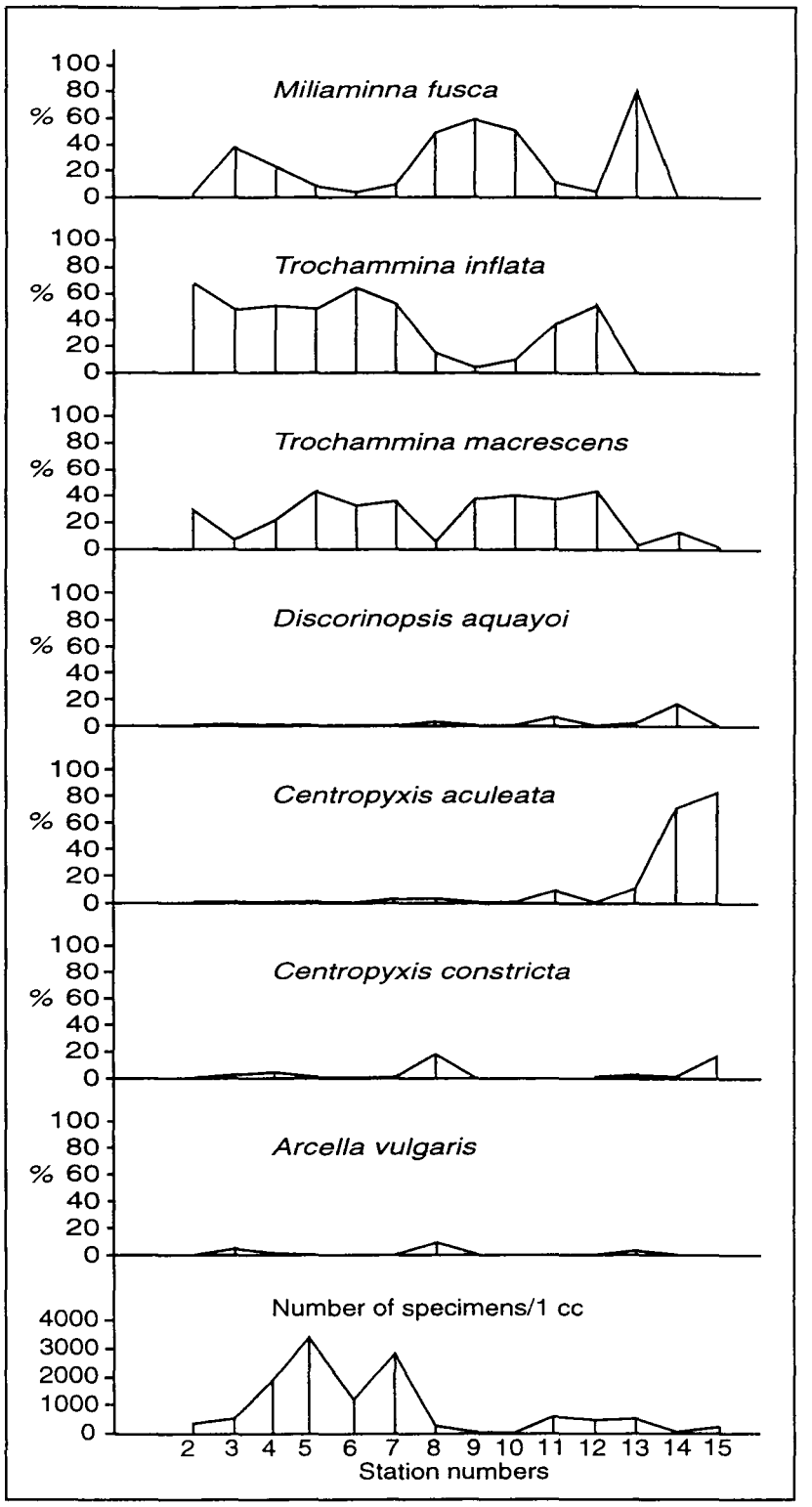

Figure 2.3: Foraminiferal and thecamoebian relative abundance for the surface transect.

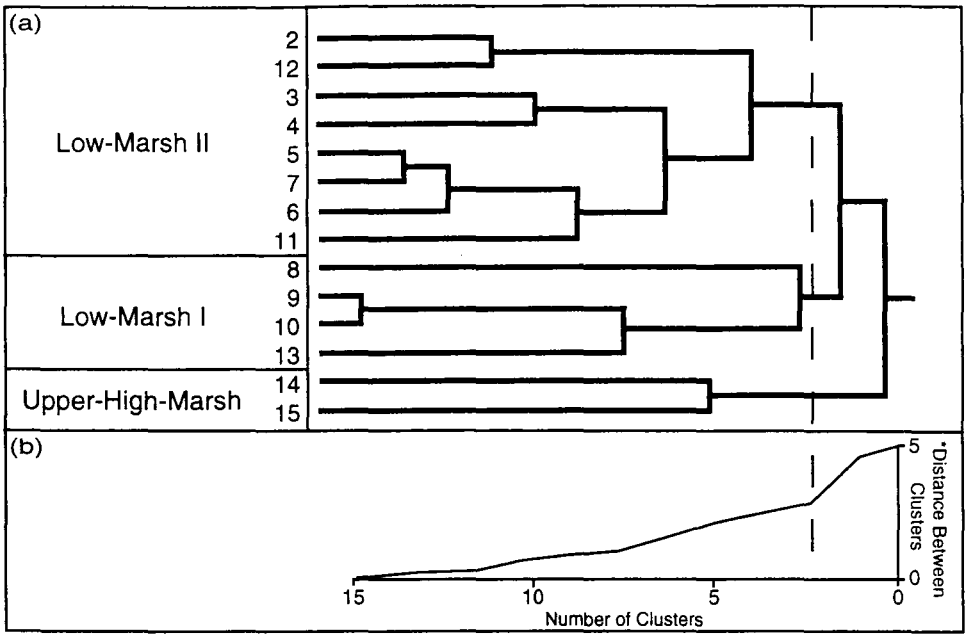

Figure 2.4: (a) Q-mode dendogram tree diagram for surface transect samples. Numbers 2 - 15 indicate sampling station number. Three clusters were identified and labeled Upper-High-Marsh, Low marsh I, and Low Marsh II biofacies.
(b) Plot of the distances between clusters. Each point represents a cluster join. *Distance between points is the ANOVA sum of squares between two clusters added up over all the variables. The break in the plot (where the dashed line crosses the curve) is a natural cutting point for determining the number of clusters.

Biofacies	Elevation range (m)	*Ammonia beccarii "tepida"*	*Arcella vulagaris*	*Centropyxis aculeata*	*Centropyxis constricta*	*Discorynopsis aquayoi*	*Milliaminna fusca*	*Trochammina inflata*	*Trochammin a macrescens*
Upper-High-Marsh	0.02-0.29	0	0	77 ± 9%	8 ± 11%	8 ± 12%	0	0	7 ± 8%
Low-Marsh I	-0.06-0.14	×	3 ± 4%	3 ± 5%	10 ± 12%	1 ± 1%	47 ± 34%	7 ± 6%	21 ± 20%
Low-Marsh II	-0.29-0.05	×	2 ± 3%	1 ± 3%	×	1 ± 2%	13 ± 12%	52 ± 10%	31 ± 12%

Table 2.2: Average species abundance in each biofacies. × is less than 1%. ± indicates one standard deviation. Elevation range is in meters above or below mean sea-level.

Similar low marsh assemblages that do not correlate with altitude (and therefore, tidal flooding frequency) have been found by De Rijk (1995) on the East Coast of North America. De Rijk (1995) concluded that marshes with variable microtopographies, such as that of the Great Marshes, Massachusetts, will have foraminiferal distributions controlled by local spatial and temporal changes in salinity, temperature, etc., and not exclusively altitude. Despite the fact that Korphos marsh slopes gradually towards the sea, hummocks and pools within the marsh create moderate microtopographical relief. The pools trap water during flooding and become more and more saline as evaporation takes place, thus allowing them to (at least seasonally) support populations of *M. fusca*.

2.3.3 Low-marsh II biofacies

Samples 2-7 and 11-12 from the surface transect clustered in the Low-Marsh II biofacies, making it the largest of the three. Two agglutinated species, *Trochammina macrescens* and *Trochammina inflata*, dominated all samples with mean relative abundances of 31% ± 12 and 52% ± 10 respectively (Table 2). We argue here that despite the fact that trochamminids are usually found on the high marsh, foraminiferal assemblages of this cluster are not truly representative of that environment because *M. fusca*, a low marsh indicator species, was observed in every sample (mean relative abundance of 13% ± 12). Better criteria with which to recognize a high marsh assemblage include complete dominance by trochamminids and other high marsh species as well as the complete absence of low marsh foraminifera (e.g. *M. fusca*; Scott et al., 1991; Hayward and Hollis, 1994; Goldstein and Watkins, 1998).

A typical "high marsh zone" does not exist at Korphos because full tidal inundation is not allowed to homogenize the environment and remove spatial heterogeneity. In other words, in marshes where complete tidal flooding takes place, fresh- and seawater are mixed in proportions related to marsh elevation (with respect to MSL), tidal range, and freshwater availability. Distinct salinity bands develop, including a high marsh band where freshwater runoff exhibits a greater influence than in intertidal or subtidal zones. In the Korphos marsh, springs and the drainage ditch create an entirely heterogeneous environment, which is not homogenized through tidal action. Low-Marsh II biofacies at Korphos are similar to other high marsh assemblages because they are dominated by *T. inflata* and *T. macrescens*, however salinity is still high enough, at least seasonally, to support small populations of *M. fusca*.

2.3.3 Upper-High-Marsh biofacies

Dominant populations of *C. aculeata* (77% ± 9 mean relative abundance) characterized the upper high marsh biofacies (Table 2). Other significant species included *T. macrescens* and *D. aquayoi*, which made up approximately 30% of sample 14, and 1.2% of sample 15. *C. aculeata* can coexist with *T. macrescens* because of its tolerance to very weakly brackish waters. *D. aquayoi* on the other hand, is one of the few calcareous, high marsh species found in arid marshes like Korphos (Scott et al., 1996).

The highest salinity of 27 ppt. was recorded in sample 15, where *C. aculeata* and *C. constricta* surprisingly made up 98% of the assemblage (Table 1). Salinity is known to change seasonally, however, and blooms of thecamoebians during the rainy season are

likely responsible for this observation as no living thecamoebians were found in this sample.

The term Upper-High-Marsh is defined here as the transitional zone between high- and fully freshwater marsh environments. Influx of seawater from the artificial tidal channel restricted thecamoebian colonization to the upper reaches of the marsh. Without the tidal channel, fresh water from seepage and rainwater would likely have been dammed by the barrier, enabling fresh to brackish marsh or lagoon to dominate more seaward regions of the marsh.

2.4. DISUSSION

The relative importance of salinity versus elevation above mean sea level for the distribution of marsh species is a matter of current debate (Scott and Medioli, 1980; Scott et al., 1990; De Rijk and Troelstra, 1997). Tides do not flood the Korphos marsh due to a protective beach barrier and thus elevation has made little impact on species distribution. The environment here has also been anthropogenically altered since AD 1950-60 when an artificial tidal channel was created, allowing seawater to inundate the marsh (despite the beach barrier) during storms and to a lesser extent during high tides. Irregular salinity gradients originating from the channel enabled the low marsh foraminifer, *M. fusca* to colonize what would otherwise have been a fresh to only slightly brackish marsh or lagoon.

Although cluster analysis of the Korphos microfauna revealed three distinct biofacies dominated by *M. fusca*, *T. inflata*/*T. macrescens*, and freshwater thecamoebians respectively, both *M. fusca* and *T. inflata* were found together in 11 of the 14 samples. In addition, *T. macrescens* were observed in every sample that clustered in the Low-Marsh I biofacies. Results of a study on salt marsh foraminifera from South Carolina by Collins et al. (1995) also found *M. fusca*, *T. macrescens*, and *T. inflata* occurring together in all marsh zones. Similarly, in a study of earthquake subsidence in the Aegean, no significant differences between foraminiferal assemblages in modern salt marsh samples were found at all except for one taken just above the intertidal mudflat containing mudflat and shallow marine calcareous species (Cundy et al., 2000). All other marsh samples yielded

mainly *Jadammina macrescens* (equivalent to our *T. macrescens*, Appendix A) and *T. inflata*.

Reasons proposed for limited zonation at Korphos include the areally limited nature of the marsh and the lack of well-established salinity zones related to limited tidal flooding. Limestone hills enclosing the site prevent lateral and inland spreading of marsh vegetation, while microtopography, seasonal fluctuations of temperature and rainfall, and the artificial tidal channel control salinity patterns.

Therefore, the vertical ranges estimated for the three biofacies in the modern marsh (Table 2) are not directly related to the tidal range. However, they do reflect as a whole the relative position of sea-level regardless of divisions. The position of the Upper-High-Marsh biofacies in particular, at both higher elevations and in distal areas from the marine sources of water, shows promise as a sea-level indicator.

2.5 CONCLUSIONS

Foraminiferal and thecamoebian assemblage zones at the surface of Korphos marsh are organized according to unique salinity gradients produced by an artificial tidal channel running along the southern edge of the marsh and freshwater inputs from springs. Without the tidal channel, the closed environment would have been occupied by a fresh to slightly brackish lagoon or marsh supporting mixed populations of thecamoebians and high marsh foraminifera due to springwater seepage. The influx of marine water from the tidal channel however, in combination with high evaporation during the summer and precipitation during the winter, create salinity gradients that enable low marsh foraminifera like *M. fusca* to inhabit non-tidal environments as far as 110m from the gulf.

Low-Marsh biofacies identified through cluster analysis were split into two subgroups: Low Marsh biofacies I consisting of greater than 50% *M. fusca*, and Low-Marsh biofacies II, dominated by *T. inflata* and *T. macrescens* with lower abundances of *M. fusca*. Low-Marsh biofacies I characterized those environments with more stable salinities, able to support dominant populations of *M. fusca*. Low-marsh biofacies II zones were on the other hand, observed in areas where salinities were less regular. Relative abundance of *M. fusca* in this environment fluctuated according to seasonal changes in temperature, rainfall, and seawater input during winter storms. Blooms of high marsh species such as *T. macrescens* and *T. inflata*, likely occurred during wetter periods when salinity was diluted by spring seepage and rainfall.

Thecamoebian-dominated Upper-High-Marsh biofacies were restricted to the upper quarter of the total vertical range of modern Korphos marsh deposits (0.02m to

0.29m above MSL) at approximately 1.20m inland from the beach barrier. Although thecamoebian distribution is controlled primarily by freshwater availability and not elevation above MSL, surficial patterns and environmental characteristics of upper high marsh zones are still useful in palaeoenvironmental reconstruction of similar fossil assemblages.

Humans have altered the modern Korphos marsh for the past 40 years, limiting its use for palaeoenvironmental comparison. Modern distribution patterns of thecamoebians and foraminifera can nevertheless be used to establish general environmental characteristics such as proximity to sea-level and salinity for later interpretation of subsurface assemblages. They can also be used in conjunction with other evidence from core sediments and have the potential to be quite effective.

CHAPTER 3: FORAMINIFERA AND TIDAL NOTCHES: DATING NEOTECTONIC EVENTS AT KORPHOS, GREECE

3.0 ABSTRACT

Five distinct foraminiferal biofacies were identified in core sediments from Korphos marsh, located on the northwestern shore of the Saronikos Gulf, Greece: Subtidal, Low-Marsh, High-Marsh, Upper-High-Marsh, and Freshwater. Including thecamoebians in the microfossil analysis enabled freshwater peats to be identified, which are sedimentologically indistinguishable from brackish peats. Positive marine tendencies identified in biofacies distributions were used for the first time to radiocarbon date relative changes in sea-level implied by a series of discrete, submerged tidal notches and beach rock adjacent to the marsh along the coast. The relatively unaltered v-shape of each notch profile suggested that sea-level rise was rapid and episodic. A comparison between the tidal notches and beach rock and an isostatically-corrected model of sea-level for this area isolated the tectonic contribution to sea-level change and revealed that at least four of the six sea-level indicators plotted well-below predicted sea-level during subsidence. Therefore, the gradual sea-level rise of the late Holocene was interrupted by at least four sub-meter to meter-scale, step-wise increases in relative sea-level during coseismic subsidence of the Korphos marsh. The results of this study show how the combination of geomorphological and salt-marsh records have the potential to remove errors stemming from notch dating and autocompaction of marsh sediments when reconstructing local sea-level change.

3.1. INTRODUCTION

In tectonically active coastal areas, evidence of ancient shorelines in the form of marine notches and beachrock can provide useful data concerning the direction, distribution, and succession of vertical displacements. They can also lead to an estimation of the recurrence interval of major earthquakes. Determining the age of these events is difficult however, especially when such features become submerged during coastal subsidence.

Another palaeosea-level indicator comes from salt-marsh foraminifera, which are sensitive to even minor variations in sea-level due to their vertical position with respect to mean sea-level (MSL) (Cundy et al., 2000). A distinct facies change from a less marine to more marine foraminiferal assemblage for example, indicates marine flooding due to a sudden rise in relative sea-level, possibly during marsh subsidence. In addition, sedimentological and foraminiferal evidence allows dating and correlation of sea-level variations, providing data with which to construct a relatively continuous record of relative sea-level change. Autocompaction during marsh sediment accretion however, can alter the original elevation of the marsh flooding horizon and decompaction models are difficult to develop.

Considering the limitations of using evidence from either geomorphological indicators or salt-marshes to reconstruct relative sea-level histories, this study will attempt for the first time, to correlate and radiocarbon date marine notches (which do not

suffer from compaction) with adjacent marsh stratigraphy and the foraminiferal record (which can be dated). Relative sea-level stands will then be compared to an isostatically modeled sea-level curve of the area to determine and date neotectonic events.

3.1.1 The Study Site

Korphos marsh is located in the southeastern Korinithia, along the western shores of the Saronikos Gulf (Fig. 1). This particular coastal wetland was selected as part of a larger project to identify pre-historic or poorly documented earthquakes in Korinthia at sites where meter-scale coseismic elevation changes have occurred.

Archaeological sites scattered along the coastline of the larger region of the Korinthia provide evidence for rapid sea-level change during the late Holocene; Kenchreai and Lechaion harbors in particular, are oft-cited examples of tectonic disruption of important trade routes in ancient Greece (Pirazzoli et al., 1996; Scranton et al., 1978). The ancient foundations of Lechaion, situated along the Korinthiakos Gulf, for example currently sit above modern sea-level while Kenchreai, located along the Saronikos Gulf, is submerged (Noller et al., 1997) (Fig. 1). Korphos Bay was a lesser-known harbor (Salmon, 1984), and likely also subject to the effects of multiple incidents of seismic activity on nearby faults (three NW-SE striking faults were observed by Noller et al. (1997) in the western and southern ends of the Korphos embayment).

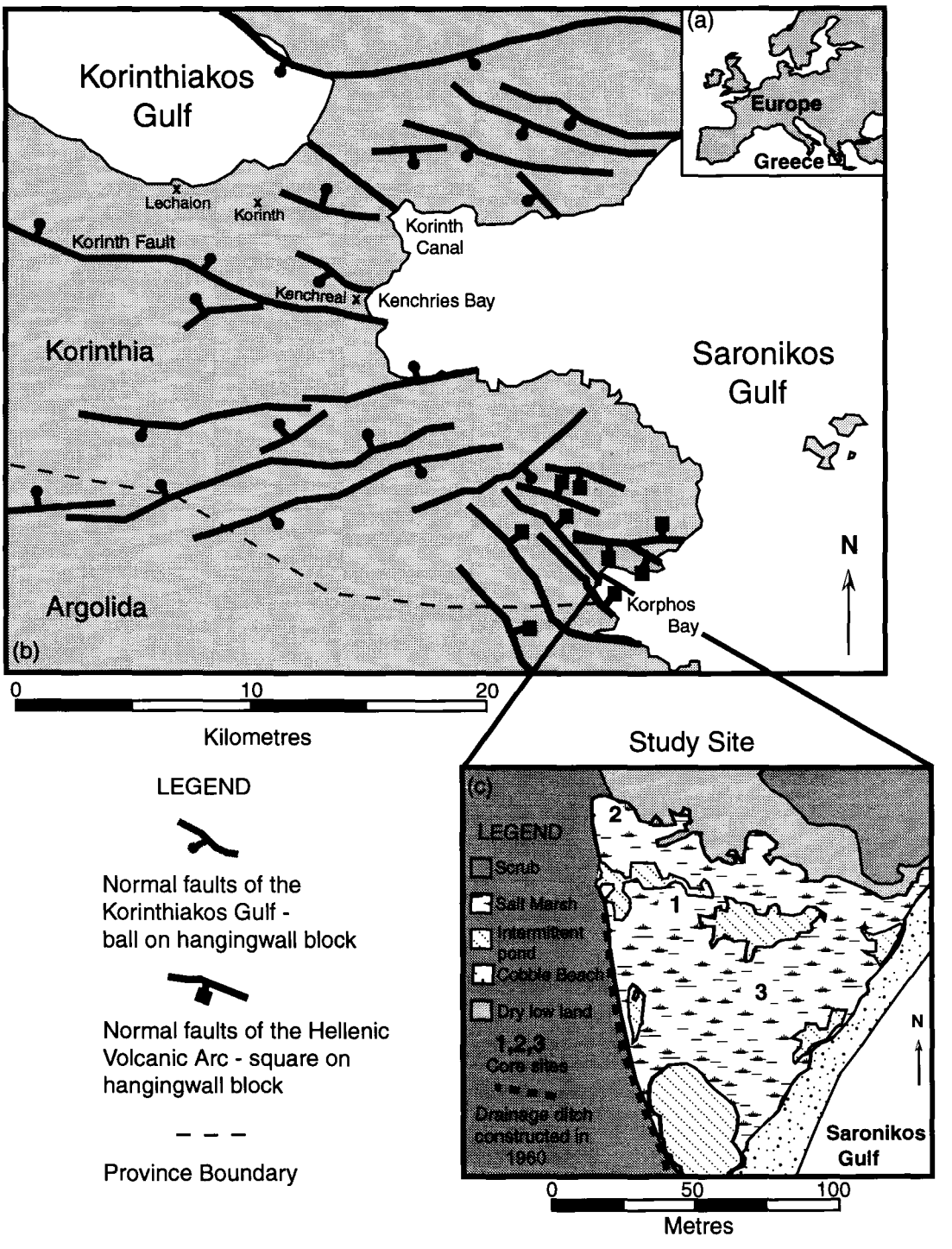

Figure 3.1: (a) Location of Greece in Europe. (b) Southeastern corner of the province of Korinthia where Korphos Bay is located. (c) Marine marsh (study site) in Korphos Bay.

The Korphos site is largely unexplored archaeologically, but Mycenean (3580-3185 ybp) and Roman (1850-1700 ybp) potsherds were observed during initial investigations of the site (personal communication from Rothaus, 2001).

3.1.2 Seismicity of Central Greece

The general pattern of faulting throughout central Greece is normal, and the overall style of deformation is roughly N-S extension balanced by crustal thinning of the Aegean subplate (Billiris et al., 1991). Regional structure is dominated by large grabens bounded by faults that affect Quaternary formations and strongly influence the pattern of drainage and sedimentation. An important characteristic of active normal faulting is that individual fault segments are rarely continuous along strike for more than about 20 km (Jackson and White, 1989). The grabens of central Greece for example, are typically bounded by fault segments that change en echeleon. This has the effect of limiting the extent of fault rupture in earthquakes, and thus, limiting the maximum earthquake size or magnitude. In the whole of Greece the individual normal fault segments in Quaternary sediments are no longer than 15 km (Stiros et al., 1992), and were probably produced by earthquakes smaller than $M_s = 6.5$ (Ambraseys and Jackson, 1990). Earthquakes have however, been numerous, of medium size ($M_s < 6.5$), and frequently preceded and followed by damaging shocks causing localized destruction (Ambraseys, 1996). The area was most

recently impacted by the series of 1981 Korinth earthquakes, which affected land level changes in the northern Peloponnesos and Korinthiakos Gulf region (Jackson et al., 1982).

The longer-term seismicity of central Greece for the period before the 17th Century is not well known. Historical data in the form of written records are unreliable, as earthquake accounts are often incomplete and perceptions of magnitude and damage are distorted. Records of earthquakes in central Greece in particular are currently inadequate for either a reasonable assessment of seismic risk or for a confident estimation of maximum magnitude (Ambraseys and Jackson, 1990). This investigation thus serves as an excellent case study for regional response to catastrophic environmental change and as a seismicity assessment for local communities.

3.1.3 Salt marshes and foraminifera

Salt marshes consist of a series of discrete levels summarized by Fletcher et al. (1993), each of which has an elevation range relative to local mean sea level (MSL). The low marsh is flooded daily by tides, and the middle marsh, flooded less often, occurs between mean high water of neap tides and mean high water of spring tides. The high marsh is located at and above the mean high water of spring tides, where freshwater runoff exhibits a greater influence, and the upland (palustrine) marsh is completely fresh. Distinct foraminiferal assemblages have been found to occupy these zones world wide

(Scott and Medioli, 1978; Patterson, 1990; Jennings and Nelson, 1992; Gehrels, 1994; Jennings et al., 1995; Nelson et al., 1996; Williams, 1999; Edwards and Horton, 2000).

Due to the close relationship between marsh elevation and local MSL (Cundy et al., 2000), coastal wetlands are particularly sensitive to sea-level change. This sensitivity has led to a number of studies which have used lithological and microfossil signatures in coastal sedimentary sequences along tectonically active plate-boundary coastlines as indicators of past earthquakes (e.g. Clague and Bobrowsky, 1994; Long and Shennen, 1994; Mathewes and Clague, 1994; Atwater et al., 1995; Hemphill-Haley, 1995; Nelson et al., 1996). Accelerations in the rate of sea-level rise relative to the rate of marsh surface aggradation for example, will result in marine flooding of the marsh and deposition of lower intertidal or subtidal foraminifera on the marsh surface. This creates a facies contact of freshwater or high marsh peats with their characteristic microfossil assemblage overlain by low marsh, tidal flat or subtidal marine assemblages (Fletcher et al., 1993). Elevation with respect to sea-level of these facies contacts may be altered in core stratigraphies however, due to autocompaction (i.e. settlement of marsh peats and clays) during sediment accretion (Kaye and Barghoorn, 1964; Cahoon et al., 1995). The oldest (and deepest) sediments are the most affected unless they were deposited directly on bedrock.

Benthonic foraminifera are useful for sea-level studies because they are relatively abundant (up to 3500 specimens per cc of sediment observed in modern samples, Chapter

2) and large enough not to be transported around by gentle current and tidal action (Hayward et al., 1999). Thecamoebians are freshwater microfauna of the phylum Sarcodina (class Rhizopodia) which are rarely present in brackish or marine conditions. Thus, their presence in marine sediments, in association with foraminifera, indicates the close proximity of a transition zone of freshwater/saltwater mixing (Fletcher et al., 1993).

Despite the fact that Greece has the highest seismic activity in the whole of the Mediterranean and European area (Makropoulos et al., 1984), the marine marshes remain largely unstudied with the exception of those from the Acheloos and Evinos deltas along the Gulf of Patras (Scott et al., 1979) and the Gulf of Atlanti wetlands (Cundy, et al., 2000). The objectives of this study are therefore to correlate microfossil and lithological signatures of relative sea-level change from Korphos with notch data, in order to resolve the both the ages of the notches themselves and the timing and magnitude of coseismic and postseismic crustal movements.

3.1.4 Marine notches and beachrock

A marine notch is an indentation or undercutting a few centimeters to several meters deep from bioerosion and dissolution processes in coastal rocks. Tidal notches, described by Pirazzoli (1986), form in sheltered, midlittoral zones (tidal zones) characterized by intermittent immersion by tide or waves. The precision of a tidal notch as a sea-level indicator increases where the site is sheltered, where the tidal range is low,

and where the cliff face is vertical; three characteristics that can be ascribed to the limestone sea cliffs at Korphos.

Notch shape is an important diagnostic tool for determining the nature of sea-level change as well. A submerged, v-shaped notch with an unaltered roof profile suggests that submergence was probably rapid and greater than the tidal range (Pirazzoli, 1986) (e.g. Notch 2 and 4, Fig. 2). A more gradual submergence between two periods of stable sea-levels on the other hand, will produce a w-shaped notch profile.

Dating notches requires that marine organisms having a distinct upper limit at sea-level (e.g. *Lithophaga lithophaga*) had encrusted or bored into the notch under study prior to rapid sea-level change (Stiros, et al, 1992; Papageorgiou et al., 1993; Vita-Finzi, 1993; Laborel and Laborel-Deguen, 1994; Pirazzoli et al., 1994; Stewart and Vita-Finzi, 1996). When relative sea-level rises or falls suddenly, it is assumed that these organisms die, leaving their shells in situ. Dates obtained from the shells should therefore reflect the timing of emergence or submergence. In the case of submergence however, modern encrusting or boring organisms that live in the subtidal zone can contaminate or completely eliminate the remains of any organisms that may have existed in the notch while it was at sea-level.

Evidence for subsidence of the coastline at Korphos was strong and included five laterally traceable, submerged, v-shaped tidal notches (Fig. 2). The notches, which were cut into limestone cliffs, ranged from 0.34 to 1.75m apart (Table 1), and are possibly

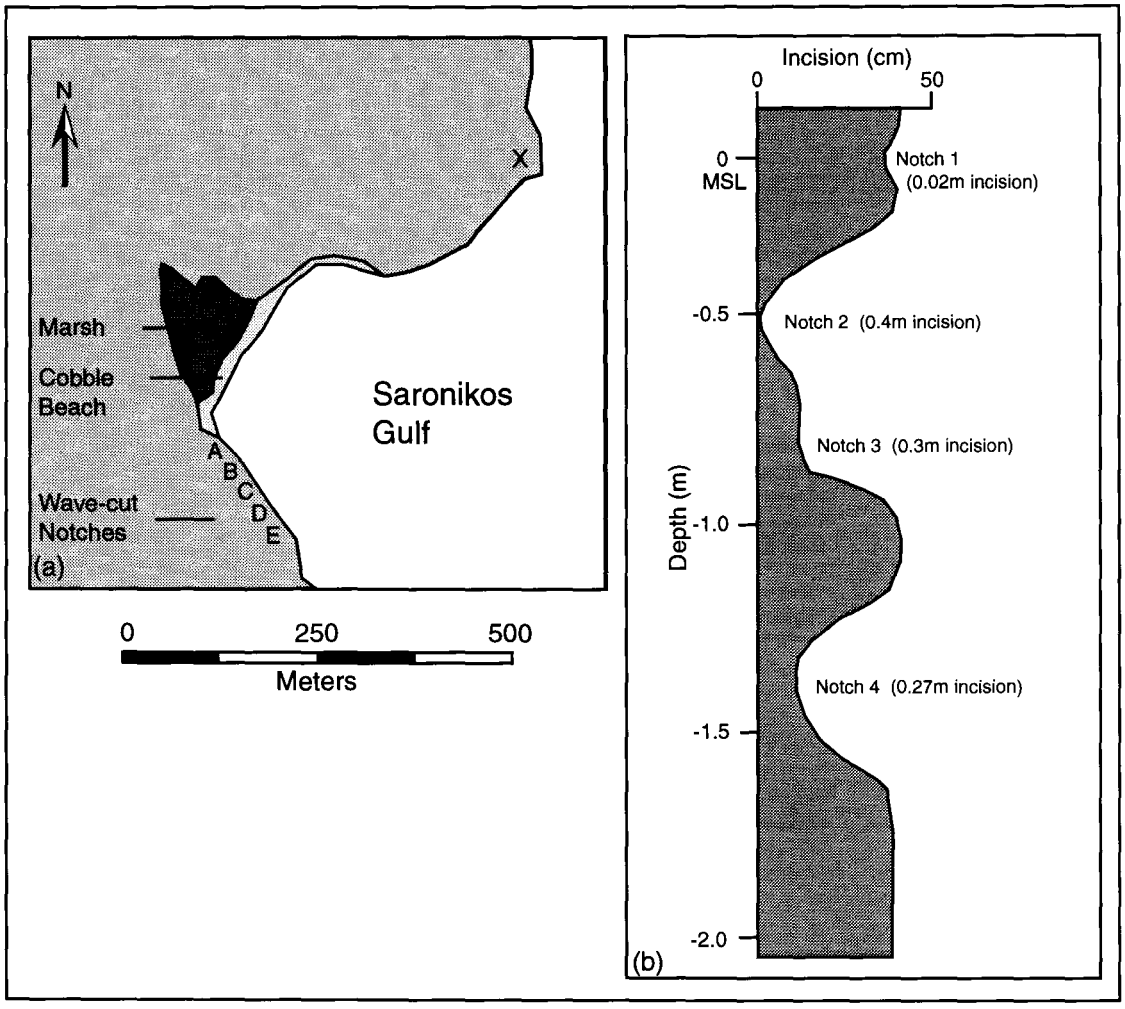

Figure 3.2: (a) Map of Korphos marsh showing locations of wave-cut notches. X marks location where submerged beach rock at -5.9m, -3.3m, -2.5m, and -1.2m were observed. (b) Example of notch profile at Site D. A submerged notch with an unaltered roof profile suggests that submergence was probably rapid and greater than the tidal range. The gently sloping roof of Notch 2 suggests that submergence was gradual rather than sudden on the other hand. The W-shaped profile of notch 2 and 3 could be indicative of a rapid submergence between two periods of stable sea-level.

Notch		Site A	Site B	Site C	Site D	Site E	Mean depth, incision & height
	Depth (middle of notch)	-0.1	-0.09		-0.1		-0.1 ± 0.1
Notch 1	incision	0.07	0.04		0.02		0.04
	height of notch	0.2	0.18		0.2		0.19
	Depth (middle of notch)	-0.37	-0.31		-0.35		-0.34 ± 0.19
Notch 2	incision	0.07	0.17		0.4		0.21
	height of notch	0.18	0.24		0.47		0.3
	Depth (middle of notch)	-0.92			-0.7		-0.81 ± 0.16
Notch 3	incision	0.24			0.3		0.27
	height of notch	0.45			0.2		0.33
	Depth (middle of notch)			-1.07	-1.32		-1.2 ± 0.22
Notch 4	incision			0.03	0.27		0.15
	height of notch			0.34	0.51		0.43
	Depth (middle of notch)					-2.94	-2.94 ± 0.16
Notch 5	incision					0.36	0.36
	height of notch					0.33	0.33

Table 3.1: A-E are notch profiles observed along the Korphos Bay coastline (Fig. 3.2). Depth units reflect mean sea-level and are in m below modern sea-level. Incision and height are in m. Mean depth error represents the tidal range based on notch height for that particular sea-level stand.

indicative of rapid and episodic sea-level changes by amplitudes that exceed the tidal range (Pirazzoli et al., 1982). Submerged beach rock at approximately -1.2, -3.3, and -5.9m and a platform at -2.5m were also observed at this location (Personal communication from Rothaus, 2001; Fig. 2). The term beach rock is applied to beach sediments found in the intertidal zone, cemented by calcium carbonate, that can form in less than a year (Hopely, 1986). The location of beach rock between the upper and lower limits of tidal oscillation makes them appealing for sea-level research (Hopely, 1975). The uppermost elevation of cementation is not always defined however, but is at least at MHWS (mean high water of spring tides). Dating beach rock is relatively easy if there is available shell material or archaeological evidence cemented into the rock. The beachrock at -5.9m was dated to ca. 3580-3185 ybp (years before present) using ages of embedded Mycenean potsherds. No dates were obtainable for the other beach rock levels.

Aside from correlating notches with archaeological evidence (Sivan et al., 2001), age estimates of coseismic and postseismic crustal movements are more easily obtained from sedimentary and fossil data found in coastal wetlands. Using subsurface littoral deposits as a dating tool for tidal notches has not been attempted before, and highlights the significance of this study.

3.1.5 Models of Holocene Sea-level Change

If confident age estimates can be made for tidal notches, they can be compared to model sea-level curves for the Holocene to verify coseismic uplift or subsidence for a given site. Exclusively using published eustatic sea-level curves for this purpose is potentially problematic (Flemming, 1972, 1978; van Andel and Shackleton, 1982) as sea-level change during the Holocene in any part of the world is a combination of eustatic, isostatic, and tectonic contributions. Isostatic effects are important in Central Greece due to the changing gravitational potential of the earth, the readjustment of the crust upon the removal of the large ice sheets, and the addition of meltwater into the Mediterranean (Lambeck, 1995). Thus, to isolate the tectonic factor, a model of sea-level for the Holocene that incorporates both the eustatic and local isostatic contributions to sea-level change is needed. Departures from this curve may be used as an argument for tectonic land level changes (Sivan et al., 2000).

Currently no isostatically corrected model of sea-level change for the Saronikos Gulf exists. However, Lambeck's (1995) curve for the Korinthiakos Gulf is a suitable alternative assuming there are no significant isostatic differences between it and the adjacent Saronikos Gulf (Fig. 1).

3.2 METHODS

Three sediment cores (4.91m, 1.37m, 3.14m in length, decompacted) were recovered from the Korphos marsh using a vibracore (Smith, 1987) that used three inch, thin-walled, steel irrigation pipes. Compaction was determined by subtracting the distance between the marsh surface and the top of the core tube from the distance between the sediment surface inside the core and the top of the tube. Compacted core lengths were 2.56m (Core 1), 1.03m (Core 2), and 1.47m (Core 3), with correction factors of 1.92, 1.33, and 2.13 respectively. Core site elevations were determined using a transit in relation to the modern tidal notch in Korphos Bay.

Microfossil samples (10cc) were taken at regular intervals in Cores 1, 2 and 3, covering all lithological units. The samples were disaggregated with a Calgon solution (25%) using a Burrel Wrist Action Shaker © and washed with a 45μm sieve to remove the silt/clay sized sediment. Due to the high organic matter content, all samples were examined wet and statistically divided for counting purposes using a wet splitter (Scott and Hermelin, 1993). Foraminiferal identification and counts were performed using a binocular microscope (× 60-95) and photographs of each species were taken using an Environmental Scanning Electron Microscope 2020 (Biology Department, McMaster University; Plate 1, Appendix A).

Samples were split into 8 equal fractions and each was examined in its entirety until at least 300 specimens were counted. In some instances, not enough specimens were

present and the entire sample was counted. A total of 44 samples were analyzed and 10 statistically significant thecamoebian and foraminiferal species were found (Table 2, 3, and 4). To gauge the uncertainty on species abundance, standard error calculations were performed on the fractional abundances (Patterson and Fishbein, 1989). The standard error was calculated using the following equation and reported in Appendix B:

$$SX_i = [X_i(1 - X_i)/N]^{1/2}$$

where SX_i is the standard error; X_i is the estimated fractional abundance for each i = 1, 2, 3, ..I species; where I = the total number of species in a particular sample; i is each species; and N is the total number of specimens counted in a sample. When making N counts the actual fractional abundance f_i lies between,

$$X_i - 1.96\ SX_i \leq f_i \leq X_i + 1.96\ SX_i$$

95% of the time regardless of the number of the species contained in the sample. The 95% confidence interval on the estimated fractional abundance is therefore

$$X_i \pm 1.96\ SX_i.$$

Q-mode cluster analysis was performed on the data set using the statistical package SAS JMP v.3 on a Power Macintosh (7300) personal computer. The resulting hierarchical dendrogram divided the samples into disjoint sets and was used to determine the various biofacies present within the three cores. This methodology approaches the Error Weighted Maximum Likelihood (EWML) clustering method of Fishbein and Patterson (1993). Cluster analysis on the relative abundance of the 10 species in the 42

Depth (m)	0.29	-0.04	-0.15	-0.29	-0.34	-0.54	-0.71	-0.90	-1.44	-1.65	-1.84	-2.04	-2.31	-2.50	-2.73	-2.82	-2.98	-3.12	-3.73	-3.98	-4.12	-4.43
Biofacies	HM	UHM	HM	HM	HM	LM	UHM	HM	-	FW	FW	FW	FW	FW	FW	FW	UHM	S	FW	S	FW	FW
Specimens per 1 cc	707	160	1142	932	168	30	1233	800	-	69	30	58	15	117	57	167	25	29	45	16	91	61
Total Counts	330	307	428	393	420	44	925	300	0	416	320	261	188	358	342	665	412	440	464	280	404	339
Ammonia beccarii "tepida"	-	-	-	-	-	-	-	-	-	-	-	4	20	×	2	5	16	48	2	38	1	-
Arcella vulgaris	-	-	-	-	-	-	-	-	-	7	-	-	-	-	-	-	-	-	-	-	-	-
Centropyxis aculeata	5	54	-	-	17	27	×	-	-	93	90	93	67	94	95	87	44	45	96	63	93	93
Centropyxis constricta	2	-	-	-	-	10	-	-	-	-	-	4	7	4	4	7	-	-	2	-	4	3
Difflugia oblonga	-	-	-	-	-	-	-	-	-	-	-	-	-	-	-	-	-	-	-	-	-	-
Discorinopsis aquayoi	-	-	-	-	-	-	-	-	-	-	-	-	-	-	-	-	-	-	-	-	-	-
Miliammina fusca	5	-	-	-	×	27	-	-	-	-	-	-	-	-	-	-	-	-	-	-	-	-
Textularia earlandi	-	-	-	-	-	-	-	-	-	-	-	-	-	-	-	-	-	-	-	-	-	-
Trochammina inflata	45	23	47	73	58	37	4	51	-	-	10	-	-	×	-	×	-	4	-	-	-	2
Trochammina macrescens	43	24	53	28	24	-	95	49	-	-	-	-	7	-	-	×	40	4	-	-	1	2

Table 2.2: Core 1 species abundance per sample, per cc. Biofacies designation as defined through cluster analysis.
HM = High Marsh; UHM = Upper High Marsh; FW = Freshwater; LM = Low Marsh; S = Subtidal.
× = less than 1% abundant.

Depth (m)	0.15	0.07	-0.07	-0.27	-0.31	-0.44	-0.57	-0.74	-1.11
Biofacies	HM	UHM	FW	HM	HM	HM	HM	UHM	UHM
Specimens per 1 cc	693	7701	40	3718	1105	2249	1179	23	141
Total Counts	520	361	352	697	420	566	444	184	423
Ammonia beccarii "tepida"	-	-	-	-	-	-	-	-	-
Arcella vulgaris	-	-	-	-	-	-	-	-	-
Centropyxis aculeata	-	28	100	-	14	3	4	52	61
Centropyxis constricta	-	6	-	-	-	-	×	17	7
Difflugia oblonga	-	-	-	-	-	-	-	-	-
Discorinopsis aquayoi	-	-	-	-	-	-	-	-	-
Miliammina fusca	1	-	-	1	×	×	-	-	×
Textularia earlandi	-	-	-	-	-	-	-	-	-
Trochammina inflata	44	11	-	68	38	43	39	9	×
Trochammina macrescens	54	56	-	31	49	54	56	28	31

Table 2.3: Core 2 species abundance per sample, per cc. See Table 2.2 for caption.

Depth (m)	0.14	0.02	-0.09	-0.22	-0.36	-0.61	-0.83	-1.26	-1.80	-2.16	-2.22	-2.33	-2.82
Biofacies	LM	HM	HM	S	S	S	S	FW	FW		FW	FW	FW
Specimens per 1 cc	837	702	1320	680	586	41	126	62	20	0	115	1	165
Total Counts	330	340	990	510	439	160	504	248	40	0	360	9	496
Ammonia beccarii "tepida"	-	-	-	93	84	49	54	16	20	-	4	-	22
Arcella vulgaris	-	-	-	-	-	-	-	-	-	-	-	-	-
Centropyxis aculeata	29	-	5	×	1	7	21	58	80	-	93	100	68
Centropyxis constricta	3	-	-	-	-	-	-	-	-	-	3	-	7
Difflugia oblonga	-	-	-	-	-	-	-	3	-	-	-	-	-
Discorinopsis aquayoi	-	-	-	-	×	-	-	-	-	-	-	-	-
Miliammina fusca	1	4	×	×	-	-	2	-	-	-	-	-	-
Textularia earlandi	8	-	-	×	-	2	-	-	-	-	-	-	-
Trochammina inflata	55	59	59	3	10	27	22	16	-	-	-	-	-
Trochammina macrescens	5	37	36	2	5	15	2	7	-	-	-	-	3

Table 3.4: Core 3 species abundance per sample, per cc. See Table 3.2 for caption.

core samples (two were not included as they contained zero specimens) isolated 8 distinct clusters.

Five of the clusters were labeled as Freshwater, Upper-High Marsh, High-Marsh, Low-Marsh, and Subtidal biofacies according to their dominant foraminiferal or thecamoebian species. Samples C1 (-1.65m), C3 (0.14 m), and C3 (-1.26m) clustered by themselves. Sample C1 (-1.65m) consisted of 93% thecamoebians, and was therefore placed in the Freshwater Biofacies. Sample C3 (0.14m) contained at total of 60% high marsh species, and was placed in the High-Marsh biofacies, while C3 (-1.26m) was put into the Subtidal biofacies due to dominant subtidal foraminifera. If the number of clusters were determined at a higher distance (see Fig. 8 for description of distance), each lone cluster (C1 (-1.65m), C3 (0.14m), and C3 (-1.26m)) would have grouped with Freshwater, High-Marsh, and Subtidal biofacies respectively.

At boundaries between biofacies, seven peat samples and one root fragment were extracted for ^{14}C dating (Table 5) and sent for analysis to Beta Analytic Inc., Miami, Florida. Two of the samples were dated using AMS, while the remaining six were dated using the radiometric technique. Dates were calibrated to calendar years using the *INTCAL98 Radiocarbon Age Calibration* program (Stuiver et al., 1998).

Grain-size analysis (for size fractions between 0.04 μm and 2000 μm) was performed using a Beckman LS Coulter Counter on samples taken at the same interval as the microfossil samples. Organic matter was removed so that only the mineralogical

Lab Number	Sample	Elevation	Sample Material	Conventional Radiocarbon Age	Calibrated Sidereal Year	Calibrated Calendar Year
Beta-153678	1	-0.08	Peat	320 ± 40	490-290	AD 1460-1660
Beta-153677	2	-0.33	Peat	280 ± 40	450-280	AD1500-1670
Beta-153676	3	-0.79	Peat	2440 ± 70	2740-2340	BC 790-390
Beta-153680	4	-2.17	Peat	2620 ± 100	2920-2370	BC 970-420
Beta-153679	5	-2.45	Peat	3920 ± 100	4780-4080	BC 2830-2130
Beta-153683	--	-3.02	Root Fragment	1870 ± 90	2000-1570	BC 50-AD 380
Beta-153682	--	-3.72	Peat	4450 ± 110	5450-4830	BC 3500-2880
Beta-153681	6	-4.31	Peat	3590 ± 90	4150-3650	BC 2200-1700

Table 3.5: Radiocarbon dates from core 1, Korphos Marsh in years BP unless otherwise stated. Error for uncalibrated dates reported as ± 1 σ. Calibrated calendar year calculated using *INTCAL98 Radiocarbon Age Calibration* program (Stuiver et al., 1998). -- Indicates that these dates were not used (discussed in text).

content of the sediments would be analyzed. Hydrogen Peroxide (30%) was used to remove organic matter and was added to each sample continuously until reactions ceased. For certain samples with a higher organic matter content, heating with a hotplate to approximately 100° C was used to hasten the reaction.

Grain-size distributions for the 44 core samples (taken at the same interval as the microfossil samples) were calculated (Appendix C) and Q mode cluster analysis was performed on this data set using the same statistical package as for the microfossil cluster analysis. The resulting hierarchical dendrogram divided the samples into 5 significant clusters, which were named Very Fine-Silt, Medium/Coarse-Silt, Coarse-Silt, Very Fine-Sand, and Fine-Sand lithofacies according to their mean grain size.

Loss on ignition (LOI) was used to determine the organic content of sediments. After oven-drying the samples to constant weight (24 hours at ca. 105°C), samples were cooled to room temperature in a desiccator and combusted to ash in a muffle furnace for 4 hours at 550°C (Heiri et al., 2000). LOI was calculated using the following equation,

$$LOI = ((DW105\ (g) - DW550\ (g))/DW105\ (g)) \times 100$$

where DW105 represents the dry weight of the sample before combustion and DW the dry weight of the sample after heating to 550°C. The weight loss is proportional to the amount of organic carbon contained in the sample.

3.3 SEDIMENTARY RESULTS

3.3.1 Organic Content

In Core 1, from the surface down to -0.71m, percent organic matter oscillated between approximately 11% and 57% varying directly with mean grain-size (Fig. 3). Below -0.71m organics decreased, ranging from 20.79% to 4.24%. A general decrease of organic content down core is typical as organic matter degrades with time. Amplitude changes in the lower section were minor and varied back and forth by approximately 4%. Some more notable transitions occurred in the -3.73m to -3.98m interval where amplitudes fluctuated between 18% and 4%, and between -2.73m and -3.12m where organics ranged from 13% to 18%. In contrast to sediments in the interval above -0.71m, sediment organic matter showed no relationship with mean grain size.

Throughout the entire length of Core 2, organic content oscillated between approximately 10% and 50% (Fig. 4). Samples with the lowest organic content also had the coarsest grain-size. Peaks in grain size at -0.07m and -0.44m for example, occurred in samples with organic contents of 13.8% and 14.5% respectively, while finer-grained samples always consisted of greater than 33.5% organic matter.

Sediments with the highest organic contents in Core 3 were observed in the near surface sediments (top 0.5m) and generally decreased down core. Fluctuations here were also fairly dramatic with high and low peaks differing by approximately 56% and 28%

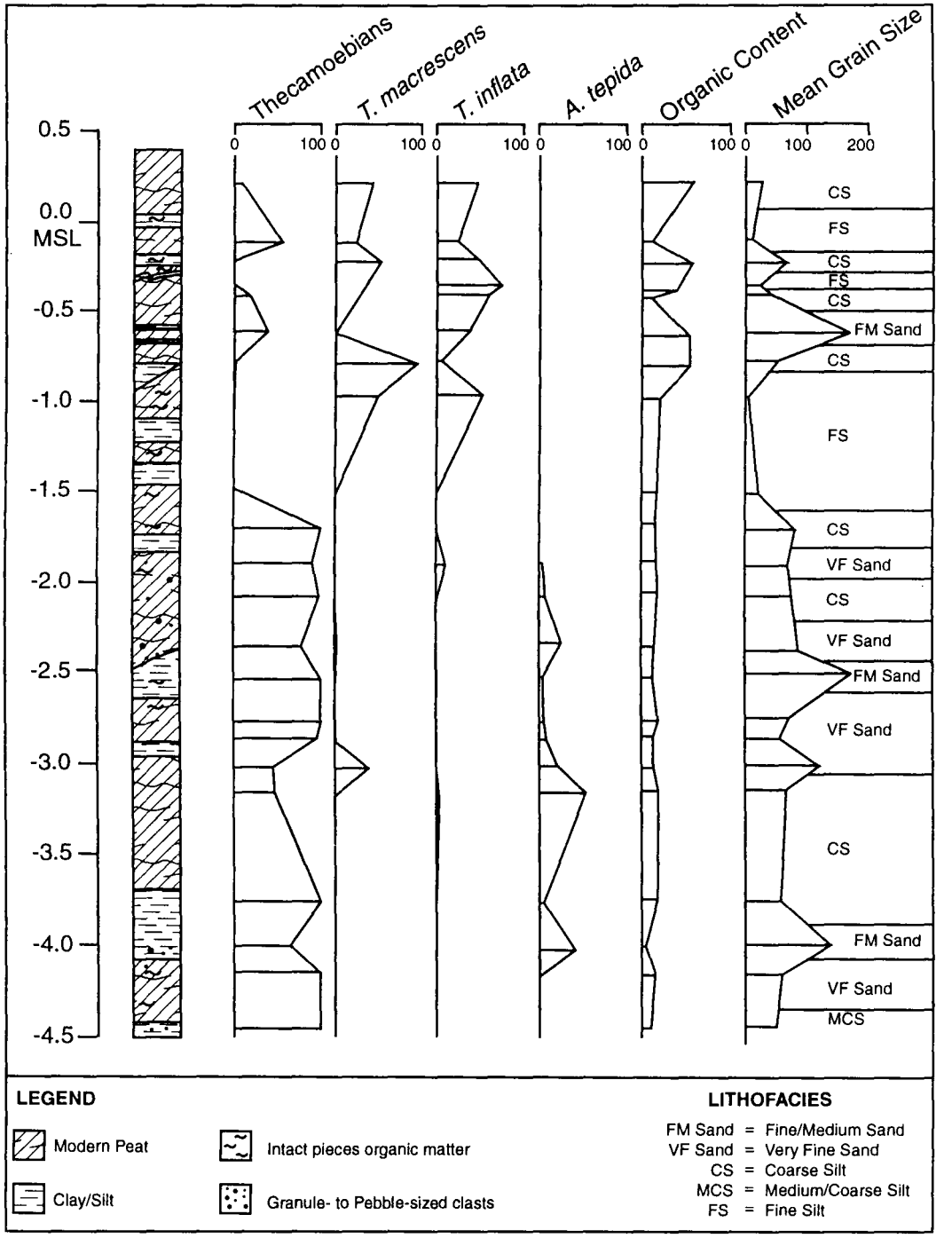

Figure 3.3: Core 1 showing species abundance, percent organic content, and mean grain size. Lithofacies were determined through cluster analysis of grain size data.

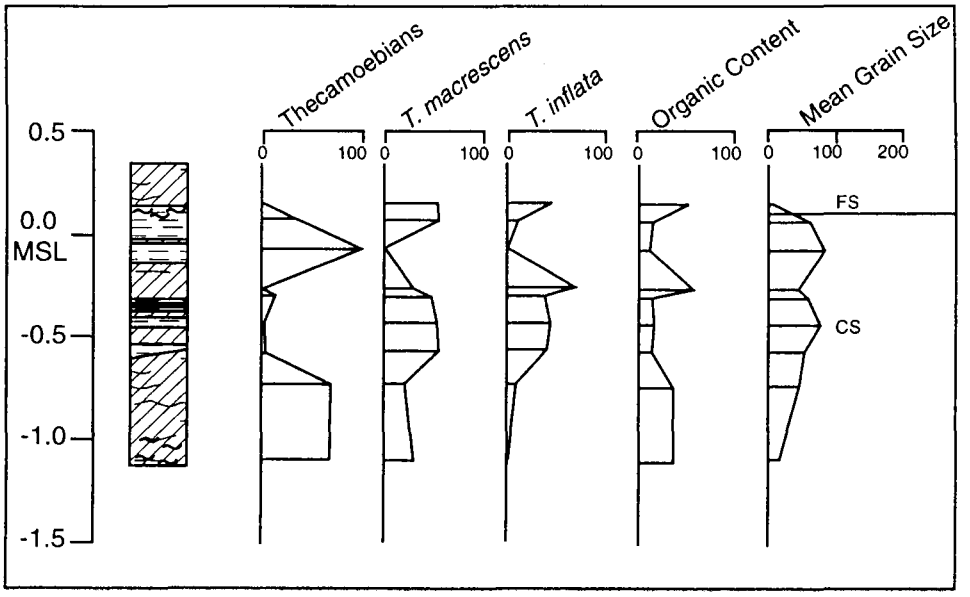

Figure 3.4: Core 2 showing species abundance, percent organic content, and mean grain size. See Figure 3 for legend.

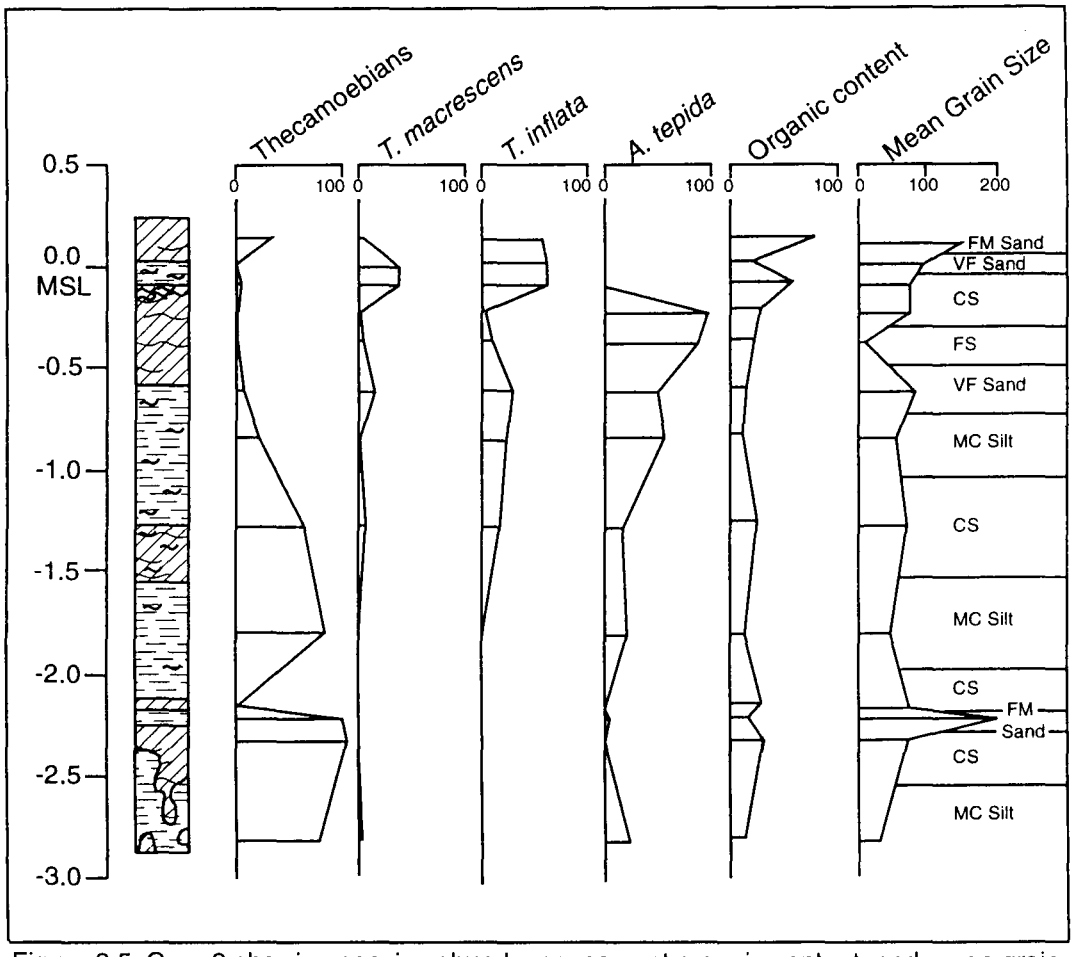

Figure 3.5: Core 3 showing species abundance, percent organic content, and mean grain size. See Fig. 3 for legend.

(Fig. 5). Low-amplitude oscillations were observed below -0.5m ranging from 11.5% to 30%.

3.3.2 Grain-Size

Cluster analysis of grain size data from the 44 core samples produced five clusters or lithofacies (Fig. 6). All samples in all lithofacies were poorly sorted (indicated by relatively high standard deviation values) over a small range of grain sizes (5.31μm to 198.9μm). The most meaningful statistic for this study was mean grain size, and lithofacies were therefore named for their Wentworth scale grain size class.

The Fine-Sand lithofacies with a mean of 166 ± 23μm (± 1σ) contained the coarsest samples that had high, flat peaks between roughly 100μm and 600μm in their grain-size distributions (Fig. 7). The Very Fine-Silt lithofacies was characterized by samples with the smallest mean grain sizes (12 ± 7μm) and low, flat-lying grain size distribution curves between 0 and 50μm. The other three lithofacies were named as follows in increasing order of mean grain size: the Medium/Coarse-Silt lithofacies (mean = 45 ± 11μm), the Coarse-Silt lithofacies (mean = 59 ± 18μm), and the Very Fine-Sand lithofacies (mean = 80 ± 21μm). Core 1 and 3 samples were present in all clusters, while Core 2 samples were only found in the Coarse-Silt and very Fine-Silt lithofacies.

Between 0.29m and -0.71m at the top of Core 1, mean grain-size of samples ranged from Very Fine-Silts to Medium-Sands (11± 14μm to 170± 152μm) (Fig. 3). A

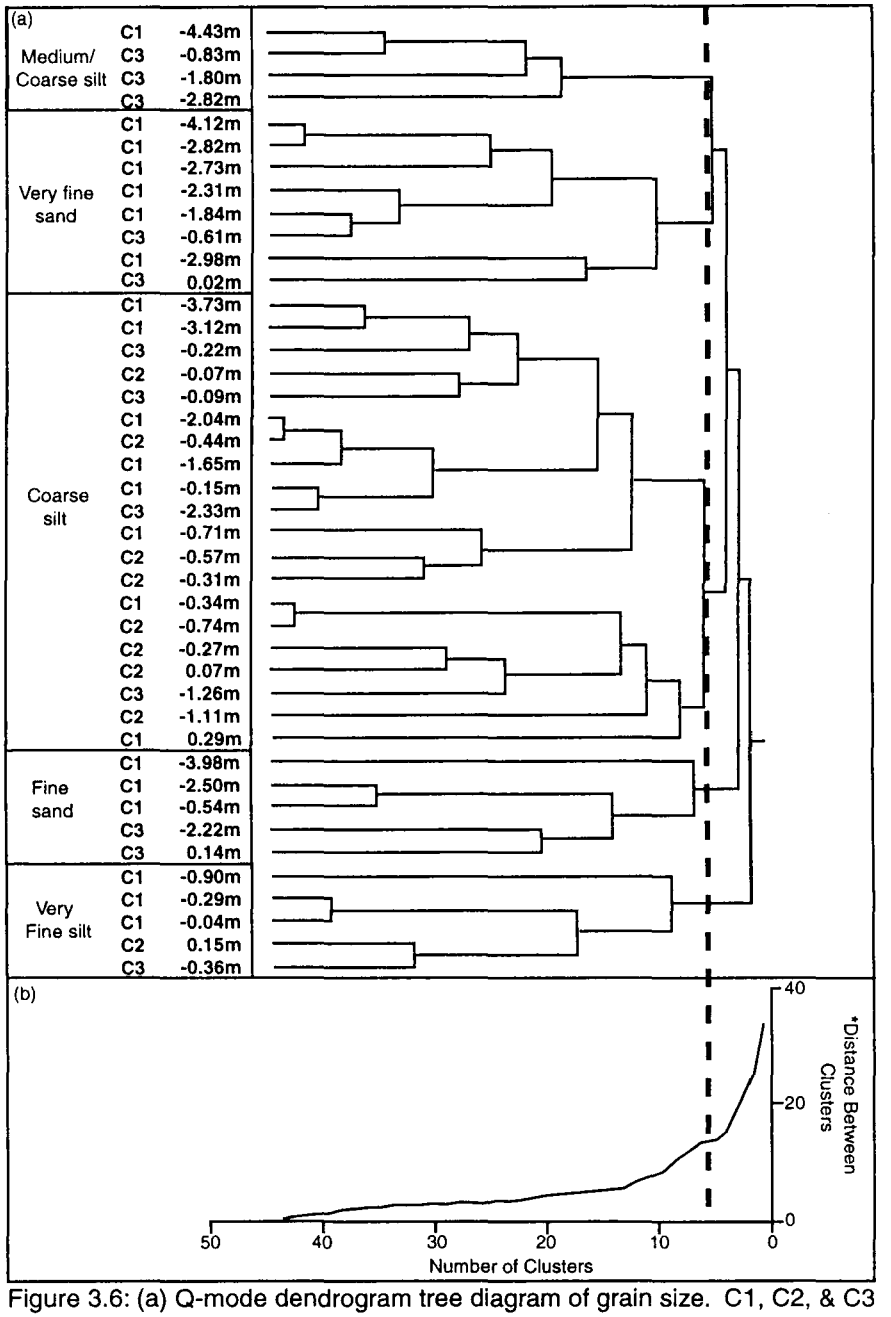

Figure 3.6: (a) Q-mode dendrogram tree diagram of grain size. C1, C2, & C3 represent core 1, core 2, and core 3 grain size samples respectively. Five clusters are shown and discerned for their average grain size according to the Wentworth scale. (b) Plot of the distances between clusters. Each point represents a cluster join. *Distance between points is the ANOVA sum of squares between two clusters added up over all the variables. The break in the plot (where the dashed line crosses the curve) suggests the natural cutting point to determine the number of clusters.

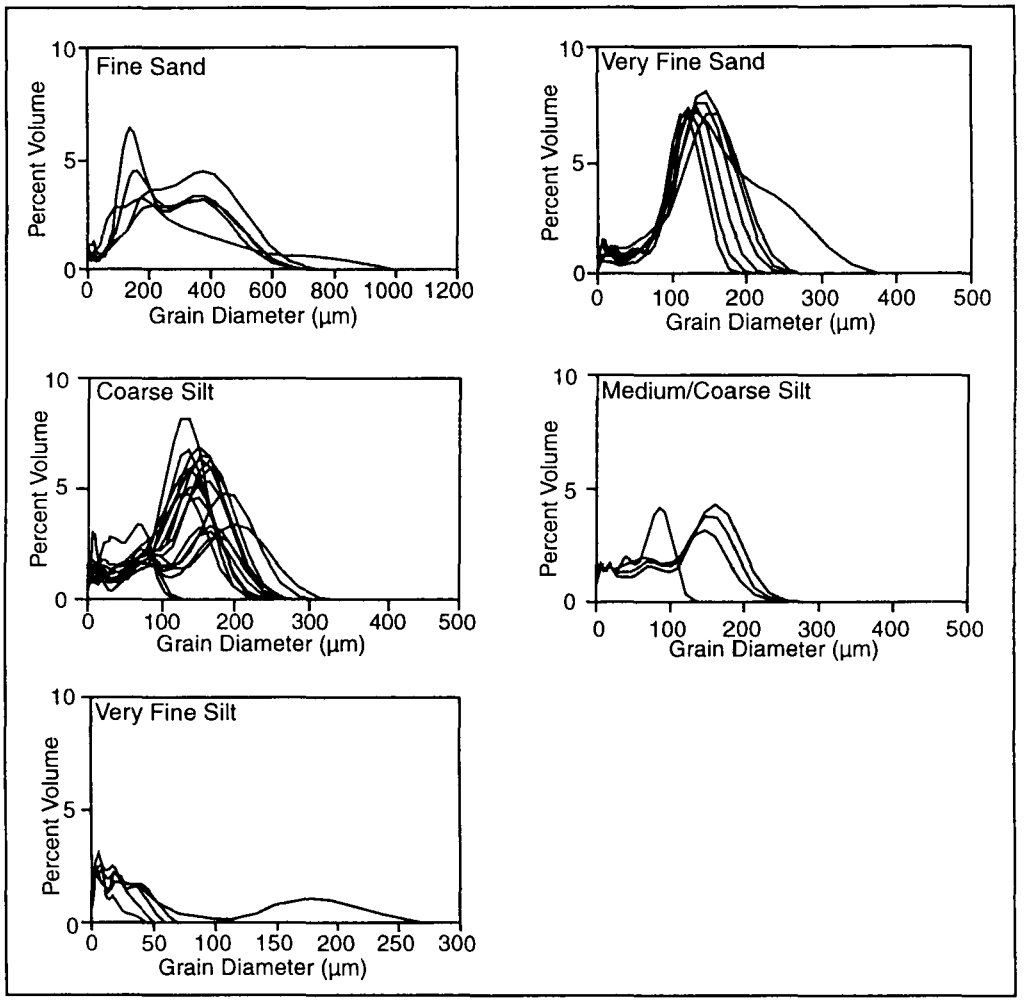

Figure 3.7: Grain Size distributions of core samples in each of the five grain size clusters.

fine-grained sediment horizon occurred between -0.9 and -1.44m, where grain-size ranged from 5.3 ± 6.6μm to 20.99 ± 6μm. Samples below -1.44m were consistently coarse, clustering in the coarse-silt and Very Fine-Sand lithofacies with two peaks of Medium-Sand at -2.5 and -3.98m.

Core 2 (taken the furthest inland) was rather homogeneous in grain size with a general decreasing trend of coarse-silts down core other than two coarser peaks at -0.07m and -0.44m (Fig. 4).

In Core 3 peaks of Fine- and Very Fine-sand occurred at the top of the core (0.14m to -0.25m), and at the bottom (-2.22m to -2.5m) (Fig. 5). Other sandy peaks were found at -0.61m and -1.26m. Only one sample at -0.36m clustered in the Very Fine-Silt lithofacies. The remaining samples were Coarse- and Medium/Coarse Silts.

3.4 MICROFOSSIL ANALYSES

Cluster analysis of the microfossil data grouped samples together that contained similar relative abundances of the different foraminiferal and thecamoebian species. These groupings were then assigned to biofacies based on the dominant taxa in the cluster and their ecological constraints (Fig. 8).

3.4.1 Subtidal Biofacies

Ammonia beccarii "tepida," dominated this biofacies with a mean relative abundance of 60 ± 22% (Table 6). *A. beccarii "tepida"* is a notably euryhaline species occupying a wide range of coastal environments. They typically live in non-vegetated inter- to subtidal areas of wetlands and brackish to hypersaline lagoons (Ozarko et al., 1997; Goldstein and Harben, 1993; Alve et al., 1999). Walton and Sloan (1990) report a general preference of *A. beccarii "tepida"* for brackish waters (broadly, 0.5 – 30 parts per thousand).

Murray (1991) described the microtidal Venice Lagoon where *A. beccarii* associations were found in all marsh environments except the higher salt marsh. In a New Zealand study, Hayward et al. (1999) found the *Ammonia* association dominant throughout the lower marsh up to a level midway between MHW (mean high water) and MHWS (mean high water spring level) where it was replaced gradually by a trochamminid association. Finding a sample with >50% *A. beccarii* was thus considered evidence for a

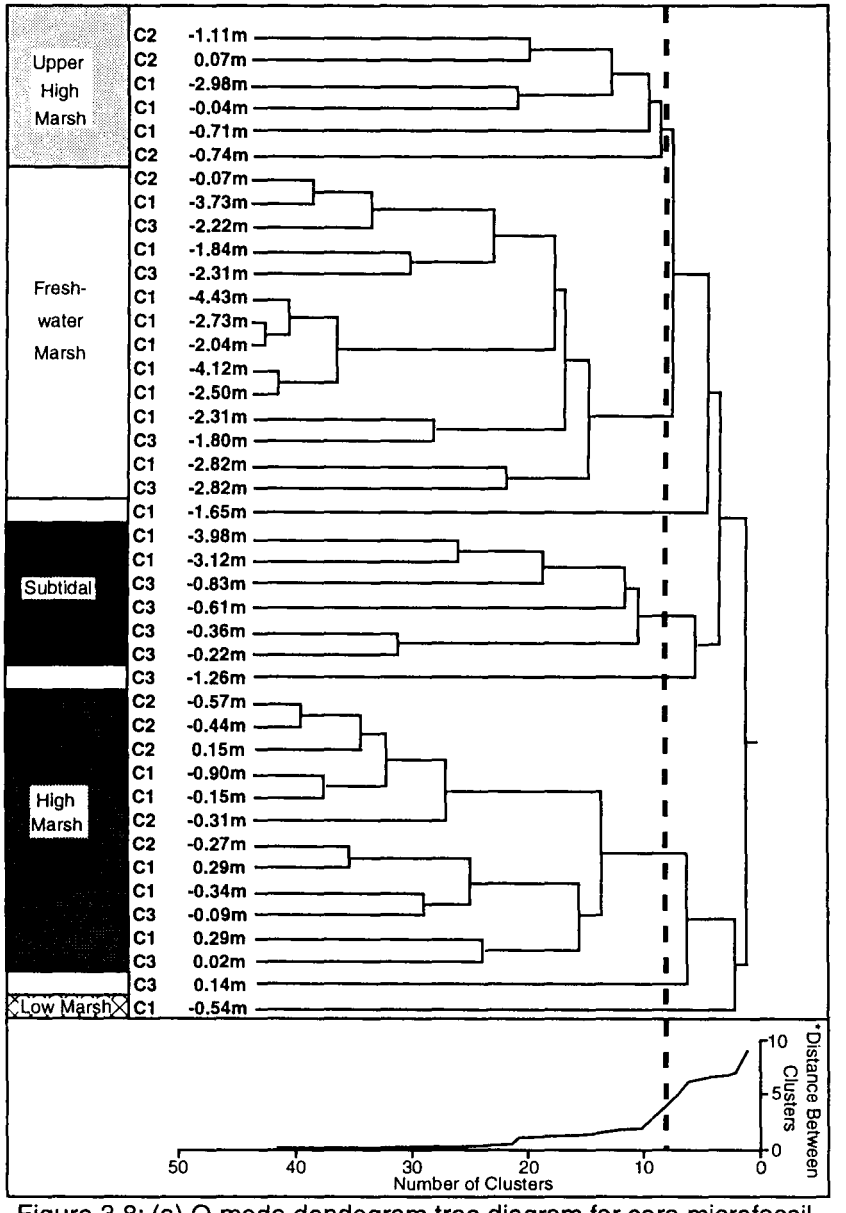

Figure 3.8: (a) Q mode dendogram tree diagram for core microfossil samples. C1, C2, & C3 represent Core 1, Core 2, and Core 3 samples respectively. Eight clusters were recognized, and labeled as Freshwater, Upper-High-Marsh, High-Marsh, Low-Marsh, and Subtidal biofacies. Colours correspond to Figure 10.
(b) Plot of distances between clusters. Each point represents a cluster join. *Distances between points is the ANOVA sum of squares between two clusters added up over all the variables. The break in the plot (where the dashed line crosses the curve) suggests the natural cutting point to determine the number of clusters.

BIOFACIES	*Ammonia beccarii "tepida"*	*Arcella vulgaris*	*Centropyxis aculeata*	*Centropyxis constricta*	*Discorinopsis aquayoi*	*Miliammina fusca*	*Textularia earlandi*	*Trochammina inflata*	*Trochammina macrescens*
Freshwater	5 ± 8%	×	83 ± 10%	3 ± 3%	0	0	0	×	×
Upper-High-Marsh	3 ± 7%	0	40 ± 23%	5 ± 7%	0	0	0	8 ± 8%	46 ± 27%
High-Marsh	0	0	6 ± 10%	×	0	1 ± 2%	×	50 ± 17%	43 ± 21%
Low-Marsh	0	0	27%	10%	0	27%	0	36%	0
Subtidal	60 ± 22%	0	23 ± 26%	0	×	×	×	13 ± 11%	5 ± 5%

Table 3.6: Average species abundance in each biofacies. × is less than 1%.

former intertidal or subtidal environment below MHWS (Hayward and Hollis, 1994; Hayward et al., 1999). In the Acheloos and Evinos deltas along the Gulf of Patras, Greece, *A. beccarii "tepida"* dominated the lowest elevations of low marsh or mudflat environments with *Protelphidium depressulum*, but were replaced by high marsh fauna *Discorinopsis aquayoi*, *Trochammina inflata,* and *Trochammina macrescens* at the margins of tidal influence (Scott, 1979).

The calcareous test of *A. beccarii "tepida"* is susceptible to dissolution after death due to the low pH of the salt marsh environment (Murray, 1971; Jonasson and Patterson, 1992; De Rijk and Troelstra, 1997, 1999). In this situation, surface assemblages with a large calcareous component are unlikely to be accurately represented in the sub-surface record although in many instances the organic linings of the tests are preserved and can be identified (Scott, 1976; Jonasson and Patterson, 1992). *A. beccarii "tepida"* is well represented Greek salt marshes however, due to buffering by the large amounts of detrital carbonate (Scott, et al., 1979).

Although there was no modern analogue for Subtidal biofacies in the surface at Korphos (Chapter 2), one of only two studies on Greek salt-marsh foraminifera found *A. beccarii "tepida"* most abundant in unvegetated environments, and scarce above the tidal range where high marsh foraminifera dominated faunal assemblages (Scott, 1979). Low sediment organic content and only minor abundances of *T. inflata* and *T. macrescens* (11

± 11% and 4 ± 5%, respectively) in Korphos samples indicate that *A. beccarii "tepida"* dominated assemblages represent subtidal environments.

C. aculeata was also present in the Subtidal biofacies with a mean abundance of 23 ± 26%. This mean however, is biased by two samples from Core 1 (44.8% in C1(-3.12m) and 62.5% in C1(-3.98m)), and without these samples the mean is much lower at 7.6 ± 9%.

C. aculeata is able to tolerate only very low inputs of saline water (1-2 ppt) such as that from occasional salt spray or storm deposits, and finding it together with *A. tepida* suggests that palaeosalinities were brackish (likely <5ppt) and fluctuating. *C. aculeata* was rare in Subtidal biofacies in Core 3, possibly due to a general increase in salinity towards the sea.

Core 3 had the largest interval of Subtidal biofacies between -0.17m and -1.2m, while Core 1 had only two smaller intervals observed between approximately -3.06m and -3.4m, and between -3.86m and -4.06m. Subtidal biofacies were not found in Core 2.

3.4.2 Low-Marsh Biofacies

The Low-Marsh biofacies was restricted to only one sample (C1-0.54m), and was dominated by the low marsh indicator, *M. fusca* (27%). *M. fusca* is a commonly employed low marsh indicator that lives in the intertidal zone of salt-marshes world-wide

(Scott and Medioli, 1978; Patterson, 1990; Scott and Leckie, 1990; Jennings and Nelson, 1992; Gehrels, 1994; Horton, 1999).

Representation of Low-Marsh environments in core sediments was limited in comparison with the modern environment (Chapter 2). A drainage ditch created in 1950-60 for malaria control however, altered the system allowing communication with the Saronikos Gulf in an otherwise closed marsh. Although marine influence was still limited due to an extremely compressed tidal range (< 30cm) it was enough to allow for the establishment of *M. fusca*-dominated Low-Marsh zones.

An alternative explanation for the absence of low marsh environments in core sediments includes poor preservation of the fragile *M. fusca* test. However, *M. fusca* was observed in 13 of the 44 core samples suggesting that preservation may not be the most significant factor. The fact that most of the samples contain thecamoebians indicates that conditions may have been too fresh over the history of the marsh for *M. fusca* to inhabit the environment.

3.4.3 High Marsh Biofacies

Eighteen samples representing each of the three cores and the surface transect made up the High-Marsh biofacies (Fig. 8). This biofacies was almost exclusively defined by two species of foraminifera, *T. inflata* and *T. macrescens*, having a mean relative abundance of 50 ± 17% and 43 ± 21% respectively (Table 6). *C. aculeata* was the only other significant species in this biofacies with a mean relative abundance of 6 ± 10%.

According to Scott et al. (1979) and Cundy et al. (2000), elevations in the upper quarter of the tidal range are exclusively dominated by trochamminids, regardless of conditions in which the marsh deposit formed. In the Acheloos and Evinos deltas of Greece for example, *Jadammina polystoma*, *T. inflata,* and *Discorinopsis aquayoi* occupied elevations between approximately -0.1m and -0.25m above MSL, replacing lower marsh foraminifera, *M. fusca* and *P. depressulum* (Scott, 1979). A monospecific fossil fauna of *T. macrescens* may indicate an elevation even closer to EHWS (extreme high water spring level) (Hayward, Grenfell, and Scott, 1999).

Core 3, which was taken closest to the Saronikos Gulf, had only one High-Marsh interval between approximately -0.18m to 0.09m. Core 1 and 2 had a High-Marsh biofacies between -0.4m and 0.13m and -0.35 to 0.13m respectively. In addition, Core 2 had one other High-Marsh biofacies interval between -0.16m and -0.65m, which could be correlated across the marsh to Core 1. The lowest sediments with High-Marsh biofacies were observed in Core 1 between -0.73m and -1.2m. High-Marsh trochamminids were almost always observed in sediments with a high organic content (Fig. 3, 4, 5).

3.4.4 Upper-High-Marsh-Biofacies

This transitional biofacies had a particular combination of freshwater thecamoebians and brackish foraminifera that characterize the upper limits of marine

influence in the Korphos marsh (add references on this idea). The dominant species in the biofacies were *T. macrescens* (46 ± 27%) and *C. aculeata* (40 ± 23%).

Although both the High-Marsh and Upper-High Marsh biofacies had similar microfaunal assemblages, there were distinguishing features that allowed for a separation between the two clusters. *T. inflata* for example, was particularly more abundant in the High-Marsh biofacies (50 ± 17%) than it was in the Upper-High Marsh biofacies (8 ± 8%) while, *C. aculeata* was more dominant in the Upper-High Marsh biofacies (40 ± 23%) than it was in the high marsh biofacies (6 ± 10%). Other differences included the presence of *C. constricta*, which was found in samples C2(0.07m) and C2(-1.11m) in the Upper-High Marsh biofacies (6% and 7% respectively), but only observed in one High Marsh sample C1(0.29m) at 2% abundance. *C. constricta* tolerates even lower salinities than *C. aculeata* and probably represents the EHWS marsh zone or higher.

Sample C1(-2.98m) contained an anomalously high, 16% *A. beccarii "tepida"*, and although not usually present in the upper reaches of the High-Marsh, can tolerate low salinities and could represent a storm or elevated salinity due to increased evaporation.

Core 3, which was taken closest to the Saronikos Gulf, did not have any samples present in this biofacies. Core 1 had three Upper-High Marsh biofacies at -2.94m to -3.06m, -0.61m to -0.73m, and 0.13m to -0.06m. Core 2 Upper-High Marsh biofacies fell between 0.13m and MSL and at the base of the core between -0.65 and -1.11m.

Upper-High-Marsh samples were observed at the most landward portions of the modern Korphos marsh transect (Chapter 2). Sample 14 for example, comprised 71% *C. aculeata* and 13% *T. macrescens*.

3.4.5 Freshwater Biofacies

The Freshwater biofacies was the other large biofacies produced from cluster analysis with 16 samples representing all three cores. *C. aculeata* dominated this biofacies with an average abundance of 83 ± 10%. Both *C. constricta* and *A. beccarii "tepida"* occurred in eleven out of the eighteen samples with a mean relative abundance of 3 ± 3% and 5 ± 8%, respectively. As mentioned previously, *C. constricta* tolerates lower salinities than *C. aculeata*, and despite low abundance values, is significant for the environmental interpretation of this biofacies as representing a freshwater environment (palustrine marsh). The presence of *A. beccarii "tepida"* is likely indicative of an area flooded by freshwater with just enough salinity to support a small, and perhaps even seasonal *Ammonia* population. Six of the samples from the Freshwater biofacies contained either one or both of the trochamminid species but mean relative abundances were less than 1%. High marsh indicator species are often found together with dominant populations of *C. aculeata* in transitional zones between the high marsh and the more upland palustrine marsh (Lloyd, 2000).

Dominant thecamoebian populations were frequently observed in sediments with a low organic content (Fig. 3, 4, 5). This suggests that freshwater biofacies are likely

indicative of a fresh to very slightly brackish lagoonal/marsh system, rather than a fully vegetated environment.

Freshwater biofacies in Cores 1 and 3 (the two closest to the Saronikos Gulf) were restricted to elevations below -1.2m and -1.5m. The largest deposition of freshwater peats occurred between -1.2m and -2.94m in Core 1 and between -1.5m and -2.94m in Core 3. Core 1 had two basal Freshwater biofacies intervals at -4.06m to -4.5m and -3.43m to -3.83m. Core 2, furthest from the sea had one Freshwater biofacies interval between MSL and -0.13m.

3.5 RADIOCARBON RESULTS

Seven peat samples and one root fragment were sampled from Core 1 at boundaries between biofacies for radiocabon dating (Table 2). Two of the dates were not considered to be accurate as they were found to be anomalously young. The root fragment at 3.02m was considered to be intrusive from above, as it was approximately 2000 years younger than peat 0.70m above it. The peat sample from 3.72m in Core 1 was also found to be approximately 900 years older than peat below it at 4.31m. This age was not considered valid as it did not follow the pattern of the other ages, and may reflect contamination by older carbon (Stanley, 2000).

The remaining six radiocarbon dated samples showed a step-wise pattern over the past 5000 years moving up-core (Fig. 9). Sediment accretion rates calculated between dates 4 and 5, and between 2 and 3 were 0.1-0.24 and 0.19-0.24 mm/yr respectively. With sediment autocompaction these are underestimates, however they are comparable to those observed in freshwater and high marsh environments, which range from 0.04 - 0.4 mm/yr (Khalequzzaman, 1989; Orson et al., 1990). Sediment accretion rates for inter- to subtidal environments on the other hand, may range from 2.0 to 6.6 mm/yr (Harrison and Bloom, 1977). Such rates were found for the upper 0.80m and lower 1.27m of Core 1.

Overlap between dates 5 and 6, 3 and 4, and 1 and 2 prevented accurate accumulation rates from being calculated for core intervals -2.45m to -4.31m, -0.79m to -2.17m, and -0.08m and -0.33m. It is clear however, that sediments in these intervals were

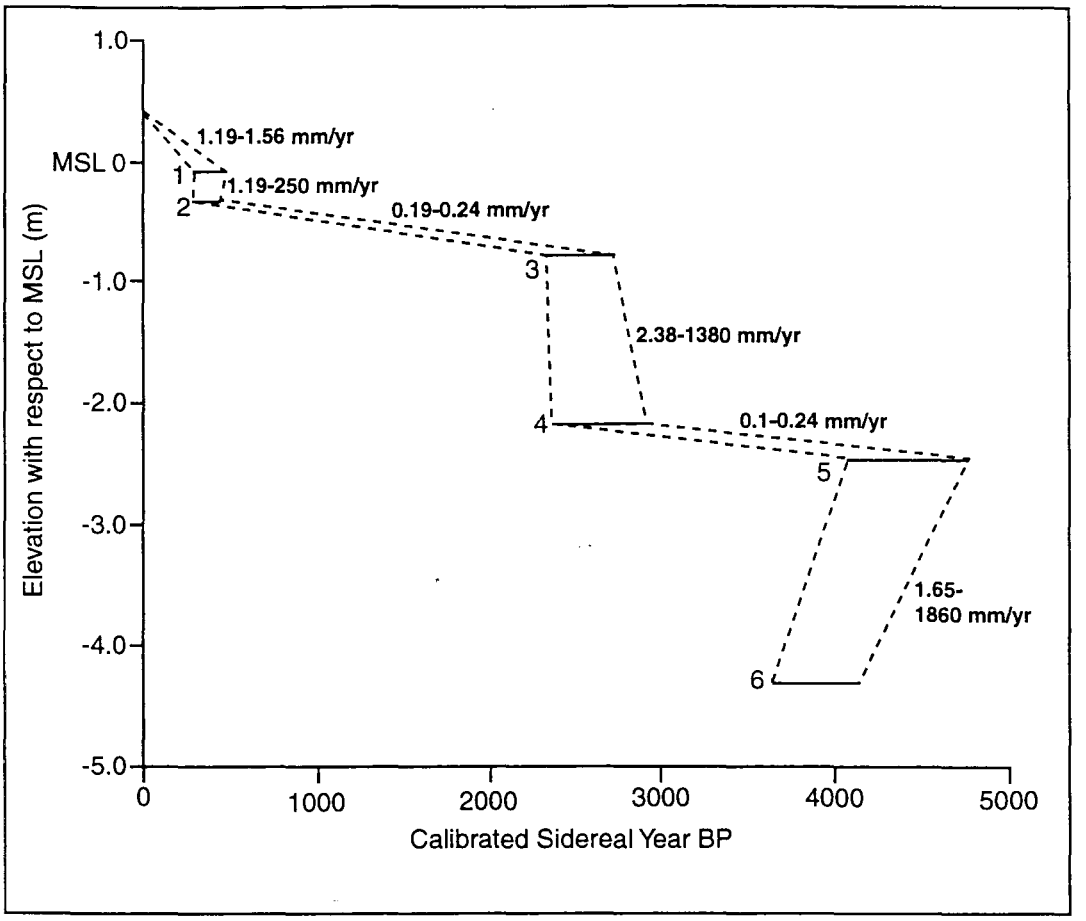

Figure 3.9: Radiocarbon dates versus depth showing rapid and episodic periods of marsh aggradation followed by more stable periods with low sedimentation rates. Numbers 1-6 indicate radiocarbon sample number (Table 2).

deposited over a relatively short period of time (4780-3650, 2920-2340, and 490-280 years bp) (Fig. 9). Age ranges were determined from upper and lower radiocarbon ages bracketing each interval. An increase in the rate of sea-level rise causes more frequent tidal flooding, which increases the rate of sediment delivery to the marsh surface (Harrison and Bloom, 1977).

3.6 DISCUSSION

Korphos marsh was subjected to six episodic coseismic subsidence events during the past 5000 years. These events were recorded as discrete tidal notches and beach rock, and in core sediments as laterally continuous, vertical facies changes indicating upward shifts to more marine influenced environments (Shennan et al., 1993; van de Plassche, 1991). Such shifts, (labeled positive marine tendency events, PMT 1-5, Fig. 10), are caused by accelerations in the rate of sea-level rise relative to marsh aggradation or by rapid marsh subsidence due to seismic activity.

Based on the results presented here, the following models were developed to depict the response of the cobble beach barrier to sea-level change and the relationships of the marsh/lagoon facies (Fig. 11). A sudden increase in sea-level for example, increases the frequency of breaching of marine water into the lagoon until the barrier builds itself back up again. During sea-level rise, barriers undergo a roll-over type response where the entire barrier migrates landward across finer lagoonal/marsh deposits without losing material (described by Cooper, 1994). According to Carter and Orford (1984), this type of barrier response during transgression is particularly effective in coarse clastic barriers (like that at Korphos).

Prior to barrier stabilization however, marsh flooding causes intertidal or subtidal biofacies to be deposited on top of existing high marsh or freshwater biofacies. Once the barrier stabilizes, preventing regular flooding of marine water other than through storms,

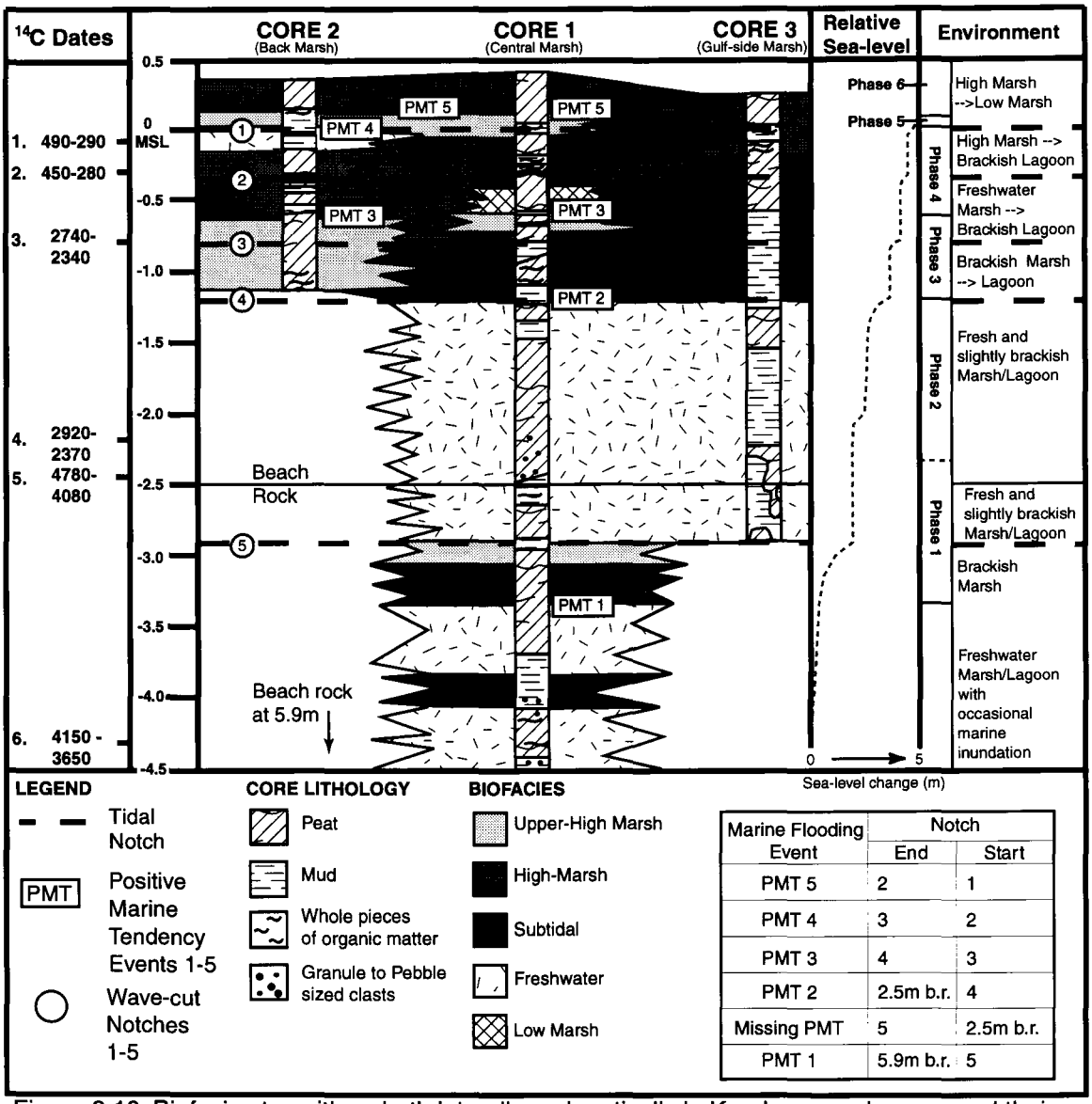

Marine Flooding Event	Notch	
	End	Start
PMT 5	2	1
PMT 4	3	2
PMT 3	4	3
PMT 2	2.5m b.r.	4
Missing PMT	5	2.5m b.r.
PMT 1	5.9m b.r.	5

Figure 3.10: Biofacies transitions both laterally and vertically in Korphos marsh cores and their relationship to tidal notch elevations. Notches and beach rock indicate former relative sea-level stands. PMT 1-5 show where marine indundation due to marsh subsidence has occurred. All ^{14}C dates in years before present. Phases 1-6 record marsh aggradation from one flooding event to the next. Dashed line between Phases 1 and 2 indicates that the marine flooding horizon is not known. Either marine inundation was not a result of subsidence at this point or biofacies recording flooding are farther seaward. Table illustrates how PMT horizons were used to determine timing of marsh subsidence. b.r. stands for beach rock.

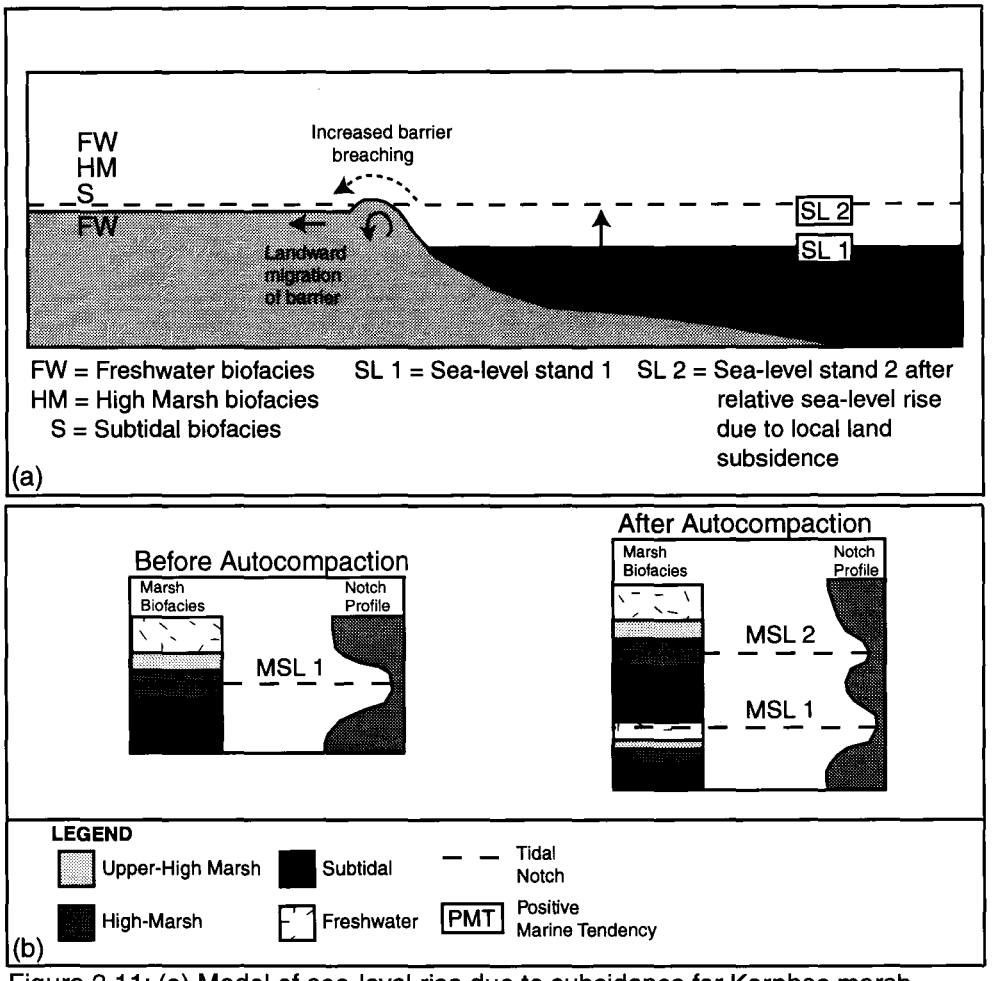

Figure 3.11: (a) Model of sea-level rise due to subsidence for Korphos marsh. (b) Model used to correlate marsh stratigraphy and tidal notches. Marsh builds above MSL (and also the tidal notch) while sea-level is stable. After sea-level rise, marsh continues building above MSL 2 and autocompaction lowers stratigraphical and biofacies contacts from MSL 1.

freshwater from seepage and rainfall becomes dammed, allowing high marsh and freshwater peats to encroach seaward. With the following event the marsh subsides and another positive marine tendency reflected in microfossil assemblages should appear above the Freshwater biofacies (SL 2, Fig. 11a).

However, correlation of the marsh stratigraphy and the tidal notches and beachrock require special consideration as autocompaction may lower PMT facies contacts in the depositional record (Fig. 11b). During notch development at a stable sea-level stand, marsh facies build upward with respect to MSL, and at Korphos, because of the stable beach -barrier, tend to "freshen upwards." That is, marsh biofacies above MSL are usually High-Marsh or Freshwater. As organic and inorganic sediments accumulate, older and lower peats and clays undergo post-depositional compaction, which results in a change of level of sediment horizons (Kaye and Barghoorn, 1964). Therefore, PMT horizons will appear at elevations below the corresponding tidal notch representing sea-level for that time period, and will gradually become more coincident moving up core and into the modern environment.

The notches were radiocarbon dated using the PMT horizons in the core. Because the PMT horizon represents a relative "instant" in time compared to the notch (which could represent hundreds to thousands of years), the age of the PMT horizon dates the end of the old notch and the beginning of the new notch (Fig. 10). The age of the notches

is limited to the range of uncertainty on the radiocarbon results. The following is a discussion of the six phases of marsh development related to subsidence events.

3.6.1 Phase 1

The first marsh subsidence event took place approximately 3853-4454 years bp according to the age of PMT 1, where microfossil assemblages recorded a sudden increase in marine influence (Fig. 10). There was no tidal notch recorded that was deeper than this PMT level. However, there was beach rock found on the other side of Korphos Bay at -5.9m that has been dated by cemented pottery to 3580-3185 years bp. The age matched quite closely the age of the PMT 1 horizon suggesting a correlation between the two. The date of the PMT 1 horizon does constrain the beginning of Notch 5 and if this date represents the end of the beach rock development then there was a 2.95m subsidence event. This seems large when the extent of the faults in the area and the magnitude of the other events recorded here are considered. There were probably other events that occurred but we have no tidal notch or beach rock representation of the event. The lower positive marine tendency at approximately -4.0m might represent one of these older events, but we had no confirmation of this based on available data.

PMT 1 was identified in Core 1 microfossil assemblages where biofacies changed from Freshwater to Subtidal. The subsequent shift to Upper-High-Marsh and eventually Freshwater biofacies represents a typical marsh aggradation sequence following a sudden

rise in sea-level (Fig. 11a). Sedimentation rates were rapid throughout Phase 1 while the marsh caught up to sea-level (Fig. 9). Trends observed in the physical characteristics of sediments at this transition such as increasing grain size and slightly decreasing organic content suggest that coarser sediments from surrounding slopes were being transported on to the marsh surface, possibly in response to the seismic activity. Growth of marsh vegetation was temporarily slowed at this time due to flooding (Fig. 3).

3.6.2 Phase 2

Following Phase 1, thick successions of freshwater peats were deposited above sea-level (Notch 5). No tidal notches were found at Korphos between Notch 4 and Notch 5, however beach rock was found at -2.5m in the opposite side of Korphos Bay (personal communication from Rothaus, 2001). This may be a reflection of an additional 0.5m sea-level rise between 4780 and 2740 years bp (which would divide this unit into two phases; Fig. 10), although evidence for marine flooding was not recorded in Phase 2 biofacies indicating that the cobble beach barrier (observed in the modern marsh) remained intact at this time due to relatively minor subsidence. We can also not rule out that sea-level could have been gradually rising at this time and the freshwater peat was simply aggrading and tracking sea-level.

In the case of rapid subsidence, both marsh and barrier must have migrated seaward preventing any marine inundation from influencing microfaunal assemblages at

this distance from the gulf (Fig. 12b). A similar interpretation was made for 6.5m of lacustrine and palustrine marsh deposits devoid of marine microfossils by Zangger (1991) for Lake Lerna, located on the Argolikos Gulf, Greece, during Holocene sea-level rise. Evidence of a gravel beach barrier in older littoral deposits towards the gulf was considered responsible for isolating the freshwater lagoon from the sea.

Peaks of fine sand were observed at -2.5m and -2.2m in Core 1 and Core 3 respectively, along with sub-rounded, pebble- to granule-sized clasts. These clasts may have fallen or been transported during the possible Phase 2 coseismic subsidence into the marsh surface via runoff or rock falls from surrounding heights.

Sedimentation rates between -2.45 and -2.94m (Notch 5) were high (1.65-1860 mm/yr), but slowed down abruptly between -2.17m and -2.45m to 0.1-0.24 mm/yr and remained as such for the next 1160-2410 years (Fig. 9). The lower interval of high sedimentation rates likely represents rapid marsh aggradation following PMT 1. Once the marsh stabilized, rates returned to those more typical of the high or palustrine marsh. Another increase above -2.17m may be a reflection of the possible rise in sea-level from Notch 5 to the -2.5m beach rock.

A long period of general stability and fresh water marsh aggradation characterized Phase 2 based on radiocarbon dates and the relatively homogeneous biofacies observed in Cores 1 and 3. The cobble beach barrier observed in the modern marsh was likely building upwards at this time, allowing natural springs and winter rains to create and sustain an

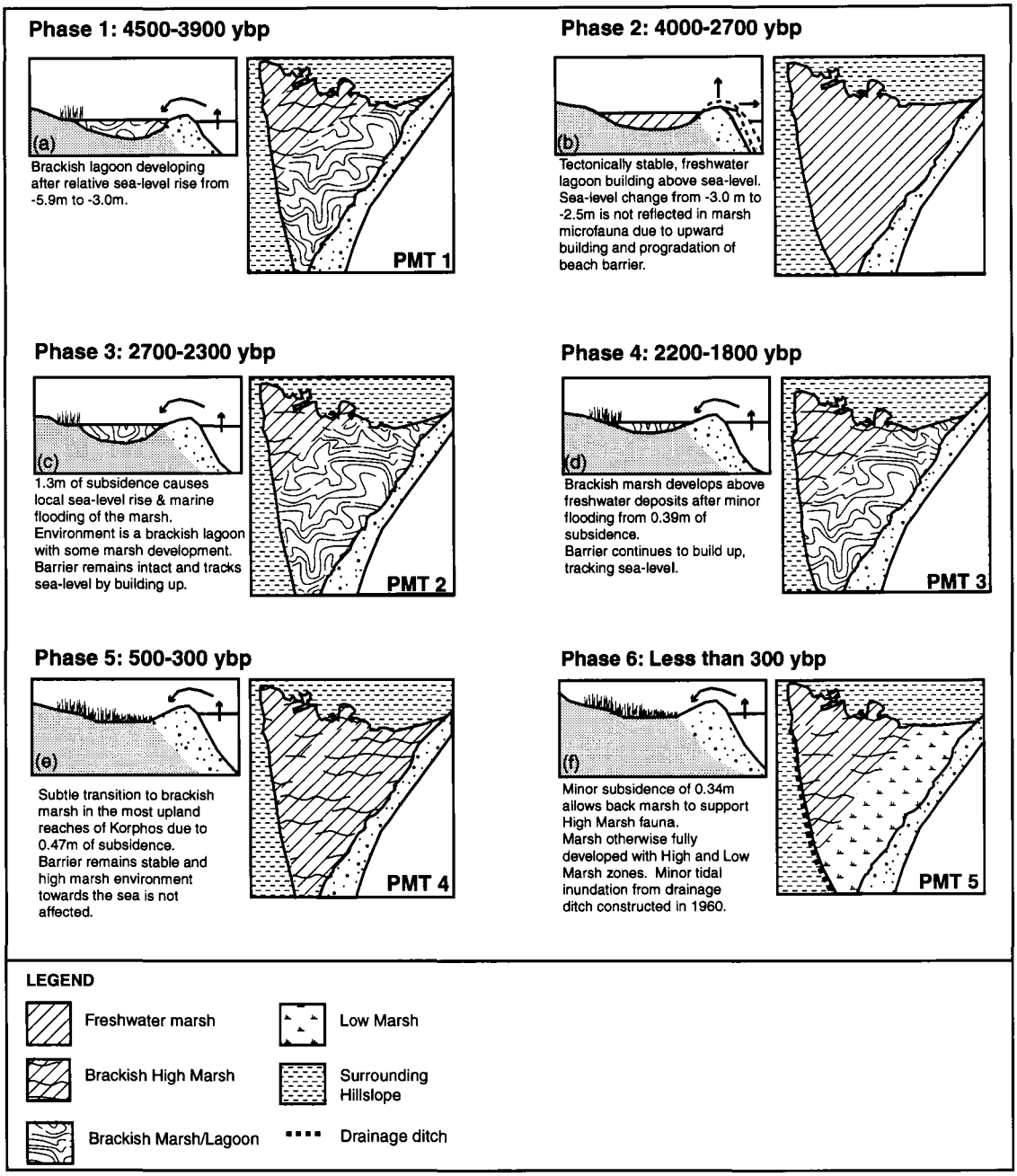

Figure 3.12: Evolution of Korphos Marsh at selected, representative times. PMT is positive marine tendency event. Phases 1-6 described in text.

elevated water table. Evidence for standing water included a lack of soil horizons and low organic content. Small populations of subtidal foraminifera (0-22% *A. beccarii "tepida"*) observed in most of the microfossil assemblages of this unit revealed that the environment was not completely fresh, and must have experienced some marine input from occasional barrier breaching during storms or seiches, or perhaps due to subsidence of Notch 5. Furthermore, the typical suites of thecamoebian species found in fully fresh marshes including *Centropyxis* and *Difflugia* species (Lloyd, 2000), were not observed at Korphos in any of the freshwater biofacies, implying that marine water was in close proximity.

3.6.3 Phase 3

In Phase 3, 1.3m of subsidence occurred and sea-level rose rapidly from the beach rock at -2.5m to Notch 4 at -1.2m. PMT 2 from this event was observed in Core 1 and 3 where Freshwater biofacies were abruptly overlain by High-Marsh and Subtidal biofacies (Fig. 10). Core 1 lithofacies shifted from Very Fine-Sands to Very Fine-Silts during flooding, while Core 3 samples remained sandy. Organic content of Core 1 sediments was initially low following subsidence but increased from 21% to 54% above 1.0m, reflecting the development of high marsh vegetation in what was previously a freshwater marsh/lagoon. In the flooded near-shore region of Core 3, organic content decreased from 25% to 12%. Sedimentation rates were very high throughout Phase 3 as the marsh attempted to catch-up with sea-level (Fig. 9).

The overall environment at this time was that of a closed, brackish marsh with a brackish lagoon towards the sea (Fig. 12c). Moving from the back marsh region into the central marsh, microfaunal assemblages shifted from Upper High-Marsh to High-Marsh biofacies, while Subtidal biofacies occupied the near-shore lagoon.

The gravel barrier was clearly breached to allow more marine flooding of the marsh surface, but remained intact, preventing regular tidal flooding and therefore the establishment of Low-Marsh zones. As both marsh and barrier stabilized, biofacies in Core 1 shifted from High-Marsh to Upper-High-Marsh biofacies. Core 3 biofacies remained Subtidal, but *A. beccarii "tepida"* abundance decreased slightly from 54% to 49%, and *T. macrescens* increased from 22% to 27% likely indicating some degree of high marsh development.

3.6.4 Phase 4

Notch 3 marked the next 0.39m of subsidence when relative sea-level rose from -1.2m (Notch 4) to -0.81m (Notch 3). Core 2 microfossil assemblages shifted dramatically from Upper-High-Marsh biofacies to High-Marsh biofacies at PMT 3. Sediments became coarser and organic content decreased with increasing marine influence. These physical characteristics of Core 2 sediments suggest that the freshwater environment below PMT 3 differed from the flooded, less organic, and more coarsely grained freshwater deposits observed between -2.94m and -1.2m in Phase 2. Upper-High-Marsh

biofacies in Core 1 lost their dominant *T. macrescens* component and gained small abundances of *T. inflata*, *M. fusca*, *T. earlandi*, and thecamoebians, *C. aculeata* and *C. constricta* (Low Marsh). Organic content and in particular, grain size, increased dramatically here as well as a low marsh environment began to develop at the edge of the near-shore lagoon (Fig. 12d). Although biofacies remained Subtidal in Core 3 sediments, high marsh foraminiferal populations decreased and *A.beccarii "tepida"* increased (84-93%) following flooding. Sediment organic content of this lagoonal environment remained low but grain-size increased, possibly due to coarser sediments being washed in during barrier breaching. The barrier itself continued tracking sea-level, building upwards and sustaining a brackish lagoonal environment immediately adjacent to the gulf (Fig. 12d).

Above PMT 3 a decrease in salinity was reflected in core biofacies. Core 2 High Marsh biofacies shifted to Freshwater biofacies while Core 1 biofacies moved from Low Marsh to High-Marsh biofacies, and the brackish lagoon inferred from Core 3 deposits finally filled in and was fully colonized by high marsh foraminifera. Organic content of Core 3 sediments accordingly jumped up from approximately 25% to 60%. Sedimentation rates were low throughout Phase 4.

3.6.5 Phase 5

PMT 4 was caused by a rise in relative sea-level from Notch 3 (-0.81m) to Notch 2 (-0.34m). Transitions in microfossil assemblages were subtle and only apparent in Core 2 (PMT 4) where Freshwater biofacies changed to Upper-High-Marsh biofacies. Marine inundation was not great enough to alter High- and Upper-High-Marsh assemblages towards the gulf (Fig. 12e). Organic content and mean grain-size of Core 2 samples did not significantly change (Fig. 4) although both variables increased slightly in Core 1 and Core 3. Sedimentation rates were very high prior to Phase 5 but decreased immediately after flooding.

3.6.6 Phase 6

The final subsidence event of 0.34m occurred when sea-level rose from Notch 2 to Notch 1 (the modern notch). Biofacies transitions were represented by PMT 5 (Fig. 10). Core 3 biofacies were not affected by subsidence, but Core 1 and 2 biofacies both shifted from Upper-High Marsh to High-Marsh (Fig. 12f). Organic content and mean grain size of sediments increased in Cores 1 and 3, but a major decrease from Coarse-Silts to Very Fine-Silts was observed in Core 2. Subsidence of Notch 2 and subsequent deposition of approximately 0.23m of sediments was rapid, occurring in less than 200 years based on the most recent radiocarbon date at 0.08m (Table 2).

3.7 SUBSIDENCE EVENTS AND PREDICTED SEA-LEVEL

To compare whether the six subsidence events described in the previous discussion were a result of coseismic vertical movement, the ages of the notches and beach rock were plotted on a corrected absolute sea-level curve for the Korinthiakos Gulf based on the glacio-hydro-isostatic model of Lambeck (1995) (Phases 1-6, Fig. 13). A curve for the Saronikos Gulf is not yet available however the Korinthiakos Gulf curve is a close approximate.

The age of the subsidence events were determined by the radiocarbon date of the PMT horizons that corresponded to sea-level rise from one notch or beach rock platform to the next. When the beach rock at -2.5m subsided by approximately -1.3m for example, PMT 2 was deposited in Core 1 and Core 3 (Fig. 10). Therefore, based on the age of PMT 2 sediments, marine flooding, subsidence of the beach rock, and the initial development of Notch 4 occurred sometime between 2337-2781 years bp.

All sea-level indicators plotted below the isostatically-corrected sea-level curve when errors on the radiocarbon dates were taken into account (Fig. 13). This indicates that the subsidence events described can be ascribed to tectonic factors since the eustatic and local isostatic contributions to sea-level change have been accounted for by the model.

Long periods of gradual sea-level rise were punctuated by short periods of sub-meter to meter-scale land subsidence. Coseismic subsidence of Notch 2 and Notch 4 (Phases 6 and 4, Fig. 13) are not as clear as they both touch the predicted sea-level

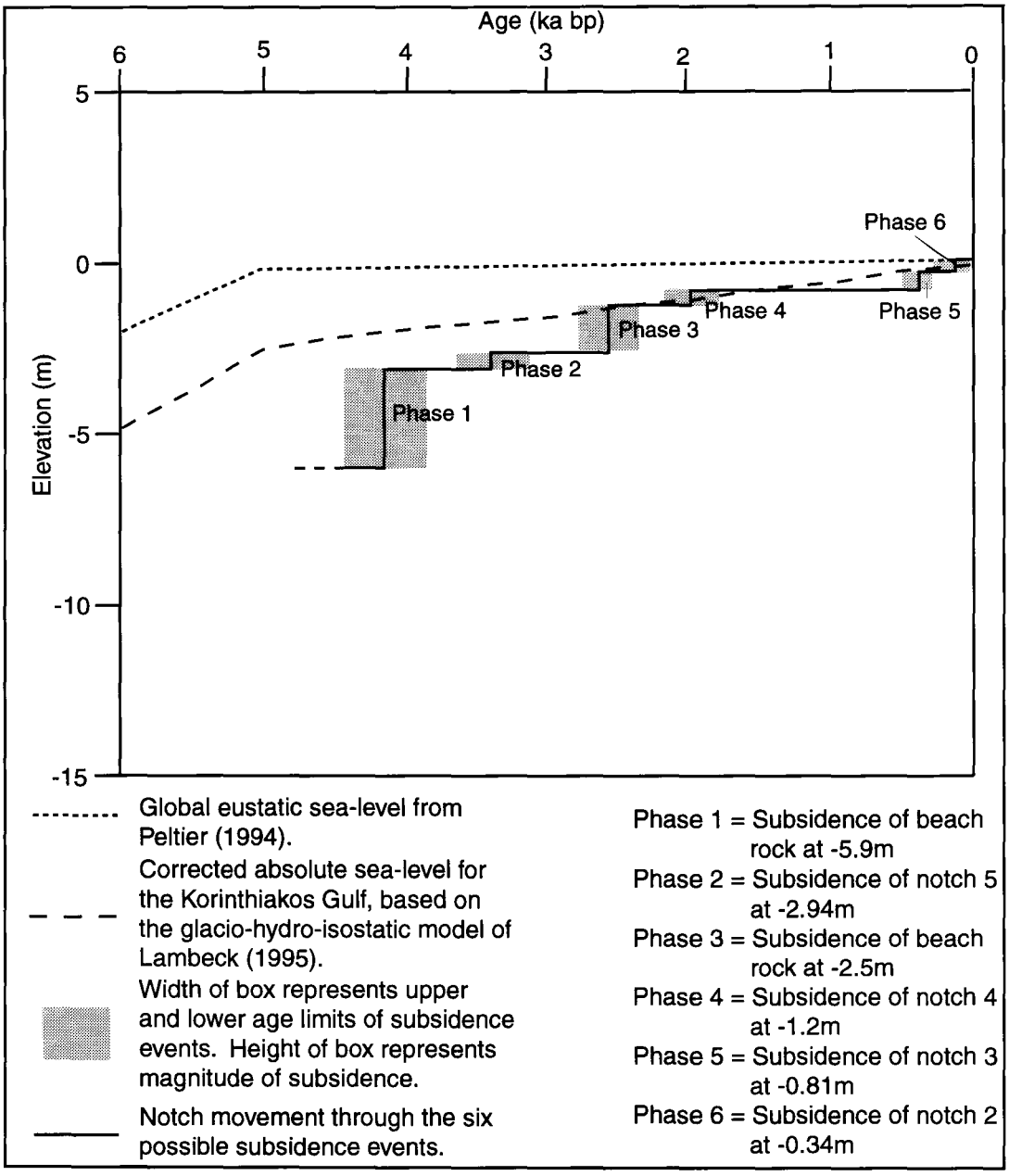

Figure 3.13: Notches and beach rock after subsidence plotted on eustatic and isostatic models of sea-level change for the Korinthiakos Gulf, Greece. All sea-level indicators plotted below the corrected curve at the time of subsidence implying that all subsidence events were tectonic in origin.

curve at their older age limits. At the younger age limits however, Notch 4 was observed approximately 0.2m lower than the predicted sea-level for that time, while Notch 3 was approximately 0.1m lower than predicted. The age range of Notch 5 subsidence could not be determined due to the absence of a corresponding PMT horizon (see discussion, Phase 2). In addition, there may be discrepancies in the model curve as our data from the notches and the PMT's indicate a seismic component.

To summarize, five rapid, meter- to submeter-scale subsidence events observed in biofacies, lithofacies, and geomorphological records from Korphos were a result of coseismic land level changes with respect to sea-level based on their positions below the glacio-hydro-isostatically corrected sea-level curve for the late Holocene. A sixth subsidence event (Phase 2, Fig. 13) which was not recorded in the microfossil record, but was recorded in the shoreface as beach rock, also indicated that sea-level was much lower than predicted, but not necessarily as a result of coseismic subsidence. Timing of this event could only be estimated relative to preceding and following subsidence events.

3.8 CONCLUSIONS

Including thecamoebians in the microfossil analysis was crucial for successful identification of positive marine tendencies in sea-level across the marsh where freshwater peats were overlain by brackish or subtidal deposits. Without the analysis of the thecamoebians, subtle transitions would not be recognized (e.g. Cundy et al., 2000). Clearly thecamoebians are an important component for unraveling sea-level histories in coastal marshes. This study also proved that different sea-level indicators (marsh stratigraphy and tidal notches) can be correlated, overcoming caveats associated with each indicator separately. By using facies transitions from salt-marsh sediments to determine the ages of the submerged tidal notches and beach rock, problems frequently encountered when using either record on its own to reconstruct sea-level change were avoided (e.g. autocompaction of marsh sediments during sediment accretion and lack of datable material for the notches). The results from this study demonstrate that this is an effective approach and should be used in other sea-level studies.

A comparison of the geomorphological evidence with an isostatically-corrected model of sea-level for the late Holocene proved to be a good method for isolating the tectonic contribution to sea-level change. The foraminiferal record and the shape of the submerged notches indicated a tectonic component, however the modeled curve acted as an important basis for comparison. Four of the six subsidence events at Korphos were

found below the curve, confirming conclusions drawn from the salt-marsh and geomorphological records. The remaining two events may have been coseismic as well, but tighter dating control is required before making this conclusion.

Based on the results presented here, coseismic subsidence event periodicity for Korphos over the time period studied was one event every 800 years. However, the last three events occurred every 600 years suggesting an increase in the frequency of events. Because the last event occurred between 300 and 500 years bp, the next event may occur within the next century. Based on magnitudes of subsidence during subsidence recognized at Korphos, the next event will likely only create offsets of a few decimeters in magnitude. Nevertheless, the town of Korphos, which is situated in close proximity to Korphos Marsh, is built less than 1.0m above sea-level and would suffer severe damage.

The results from this study are also important from an archaeological perspective. This study is part of a broader study examining linkages between coastal evolution and maritime trade patterns. In most of the other locations along the Korinthia coastline there are no marshes to correlate tidal notches with. The Korphos marsh has allowed us to both conclude that seismic land level changes are a factor in the formation of the notches and to estimate the time required for the notches to form. The modern notch took approximately 300-500 years to cut 0.04m into the limestone cliff face. This gives an estimated erosion rate of 0.09 to 0.13mm/yr as a basis for estimating the sea-level history of other sections of the coast using the tidal notches.

The sea-level history that we have developed from the Korphos marsh indicates that in the immediate vicinity Mycenean and Bronze Age archaeological sites will be as much as 5.9m below modern sea-level. This is indispensable information for the archaeologists in their search for submerged coastal sites along the western Saronikos Gulf.

CHAPTER 4: CONCLUSIONS

A cobble-beach barrier sitting 0.5m above sea-level was found to prevent regular tidal flooding in the modern salt-marsh at Korphos, Greece. The only pathway for seawater to enter the marsh other than barrier breaching during storms is a drainage ditch, which was constructed in 1950-60 to prevent outbreaks of malaria in communities situated near-by. Human alteration and the beach barrier therefore prevent distinct foraminiferal zones from establishing themselves according to elevation with respect to MSL. Foraminiferal biofacies are consequently organized at the surface according to heterogeneous salinity patterns created by the artificial tidal channel, seasonal fluctuations in rainfall and temperature, fresh water seepage from natural springs, and occasional seawater influx from winter storms.

As a result, modern biofacies could not be used as proxies for elevations above or below mean sea-level in fossil assemblages because they do not reflect a natural salt-marsh environment. Modern biofacies included Low-Marsh and Upper-High-Marsh biofacies. Low-Marsh biofacies were split into two subgroups: Low-Marsh I with greater than 50% *Miliammina fusca* and Low-Marsh II with less than 50% but greater than 0% *M. fusca*, and a high relative abundance of high marsh trochamminid species. Low-Marsh II biofacies were rare in core sediments, while Low-Marsh I biofacies were completely absent. The Upper-High-Marsh biofacies from the surface was also observed in core sediments and consisted mainly of *Centropyxis aculeata* and *T. macrescens*. The distribution of these three biofacies in the modern marsh was found useful for

establishing the broader environmental settings for similar biofacies recognized in fossil assemblages.

Biofacies without modern equivalents recognized in core sediments included Subtidal, High-Marsh, and Freshwater biofacies. Subtidal biofacies had dominant *Ammonia beccarii "tepida"* populations and represented brackish lagoonal environments based on previous descriptions of their preferred habitats in Greek coastal marshes made by Scott et al., (1979). High-Marsh biofacies with dominant trochamminid populations and a complete absence of low marsh foraminifera were considered to inhabit similar environments to Low-Marsh II biofacies from the surface but with a greater freshwater influence to keep salinities very brackish. Freshwater biofacies were completely dominated by *C. aculeata* and represented the uppermost reaches of the marsh.

Recognizing transitions in core biofacies from less to more marine environments was crucial to the success of reconstructing local sea-level for Korphos for the past 5000 years. This was accomplished by radiocarbon dating these marine flooding horizons and correlating them with discrete geomorphological indicators of past sea-levels, including tidal notches and beach rock. Using older, salt marsh sediments as a dating tool for sea-level reconstruction based on submerged marine notches and beach rock has not been attempted before, but proved successful for Korphos. The sea-level history produced by this method, which included five episodes of rapid meter- to sub-meter scale subsidence, was tested by plotting both notch and beach rock elevations and marine flooding events observed in core sediments on an isostatically corrected sea-level curve for central

Greece. Four of the six notches and beach rock platforms sat at lower than predicted sea-level stands during subsidence, confirming our initial conclusion that they were tectonic in nature. The remaining two may have also indicated subsidence depending on error, but tighter dating control is required.

Studies of this nature are particularly useful along the Saronikos coastline of the Peloponnese where little documentation of sea-level change currently exists. This is made especially clear by the fact that no isostatically-corrected model of sea-level for the Saronikos Gulf currently exists. At sites along the western Saronikos coastline where there is no salt-marsh with which to use as a dating tool for local notch profiles, results from this study (including notch erosion rates) may be used to place age estimates on events represented by notches. These results also provide indispensable information for archaeologists in their search for submerged coastal sites along the western Saronikos Gulf.

REFERENCE LIST

Allen, J. R. L. 1997. Simulation models of salt-marsh morphodynamics: some implications for high-intertidal sediment couplets related to sea-level change. Sedimentary Geology 113:211-223.

Almogi-Labin, A. 1995. Occurrence and distribution of the foraminifer *Ammonia beccarii tepida* (Cushman) in water bodies, Recent and Quaternary, of the Dead Sea Rift, Israel. Marine Micropaleontology 26:153-159.

Alve, E. and Murray, J. W. 1995. Experiments to determine the origin and Palaeoenvironmental significance of agglutinated foraminiferal assemblages. In, Proceedings of the fourth international workshop of Agglutinated Foraminifera. Edited by M. A. Kaminski, G. Stanisllaw, Gasinski, and M. Adam. Grzybowski, Poland: The Grzybowski Foundation, Cracow, Poland.

Alve, E. and Muray, J. W. 1999. Marginal marine environments of the Skagerrak and Kattegat: a baseline study of living (stained) and benthic foraminiferal ecology. Palaeogeography, Palaeoclimatology, Palaeoecology 146:171-193.

Ambraseys, N. N. 1996. Material for the Investigation of the Seismicity of Central Greece. In Archaeoseismology, edited by S. Stiros and R. E. Jones. Athens, Greece: Institute of Geology and Mineral Exploration: British School at Athens.

Ambraseys, N. N. and Jackson, J. A. 1990. Seismicity and associated strain of central Greece between 1890 and 1988. Geophysical Journal International 101(3): 663-708.

Atwater, B. F. and 15 others, 1995. Summary of coastal geological evidence for past great earthquakes at the Cascadia subduction zone. Earthquake spectra 11:1-18.

Bao, R., da Conceição Freitas, M., and Andrade, C. 1999. Separating eustatic from local environmental effects: a late-Holocene record of coastal change in Albufeira Lagoon, Portugal. The Holocene 9(3):341-352.

Billiris, H., Paradissis, D., Veis, G., England, P., Featherstone, W., Parsons, B., Cross, P., Rands, P., Rayson, M., Sellers, P., Ashkenazi, V., Davison, M., Jackson, J., and Ambraseys, N. 1991. Geodetic determination of tectonic deformation in central Greece from 1900 to 1988. Nature 350:124-129.

Bradshaw, J. S. 1968. Environmental Parameters and Marsh Foraminifera. Limnology and Oceanography 13(1):26-38.

Buzas, M. A. 1968. On the spatial distribution of foraminifera. Contributions from the Cushman Foundation for Foraminiferal Research 19:1-11.

Cahoon, Donald R., Reed, Denise J. and Day, Jr., John W. 1995. Estimating shallow subsidence in microtidal salt marshes of the southeastern United States: Kaye and Barghoorn revisited. Marine Geology 128:1-9.

Carter, R. W. G. and Orford, J. D. 1984. Coarse clastic barrier beaches: a discussion of their distinctive dynamic and morphosedimentary characteristics. Marine Geology 60:377-389.

Clague, J. J. and Bobrowsky, P. T. 1994. Evidence for a large earthquake and tsunami 100-400 years ago on the western Vancouver Island, British Columbia. Quaternary Research 41:176-184.

Collins, E. S., Scott, D. B., Gayes, R. T., Medioli, F. S. 1995. Foraminifera in Winyah Bay and North Inlet marshes, South Carolina: a relationship to local pollution Sources. Journal of Foraminiferal Research 25:212-223.

Cooper, J. A. G. 1994. Lagoons and microtidal coasts. In Coastal Evolution - Late Quaternary shoreline morphodynamics, edited by R. G. W. Carter and C. D. Woodroffe. Cambridge: Cambridge University Press.

Cundy, A. B., Kortekas, S., Dewez, T., Stewart, I. S., Collins, P. E. F., Croudace, I. W., Maroukian, H., Papanastassiou, D., Gaki-Papanastassiou, P., Pavlopoulos, K., and Dawson, A. 2000. Coastal wetlands as recorders of earthquake subsidence in the Aegean: a case study of the 1894 Gulf of Atalanti earthquakes, central Greece. Marine Geology 170:3-26.

De Rijk, S. 1995. Salinity control on the distribution of salt marsh foraminifera (Great Marshes, Massachusettes). Journal of Foraminiferal Research 25:156-166.

De Rijk, S. and Troelstra, S. R. 1997. Salt marsh foraminifera from the Great Marshes, Massachusetts: environmental controls. Palaeogeography, Palaeoclimatology, Palaeoecology 130:81-112.

De Rijk, S. and Troelstra, S. R. 1999. The application of a foraminiferal actuo-facies Model to salt-marsh cores. Palaeogeography, Palaeoclimatology, Palaeoecology 149:59-66.

Debenay, J. -P., Bénéteau, E., Zhang, J., Stouff, V., Geslin, E., Redois, F., and

Fernandez-Gonzalez, M. 1998. *Ammonia beccarii* and *Ammonia tepida* (Foraminifera): morphofunctional arguments for their distinction. Marine Micropaleontology 34:235-244.

Debenay, J. -P., Eichler, B. B., Duleba, W., Bonetti, C., and Eichler-Coelho, P. 1998. Water stratification in coastal lagoons: its influence on foraminiferal assemblages in two Brazilian lagoons. Marine Micropaleontology 35:67-89.

Devoy, R. J. N. 1987. Sea Surface Changes; where do we go from here? London: Croom Helm.

Dominey-Howes, D., Dawson, A., and Smith, D. 1998. Late Holocene coastal tectonics at Falasarna, western Crete: a sedimentary study. In Coastal Tectonics, edited by Stewart, I. S., and Vita-Finzi, C. London, U.K.: Geological Society, London, Special Publications, 146:343-352.

Edwards, R. J. and Horton, B.P., 2000. Reconstructing relative sea-level change using UK salt-marsh foraminifera. Marine Geology 169:41-56.

Fishbein, E. and Patterson, R. T., 1993. Error weighted maximum likelihood (EWML): a New statistically based method to cluster quantitative micropaleontological data. Journal of Paleontology, 67:475-486.

Flemming, N. C. 1968. Holocene Earth Movements and Eustatic Sea Level Change in the Peloponnese. Nature 217:1031-1032.

Flemming, N. C. 1978. Holocene Eustatic Changes and Coastal Tectonics in the Northeast Mediterranean: Implications for Models of Crustal Consumption. Philisophical Transactions of the Royal Society of London, Series A: Mathematical and Physical Sciences 289, no. 1362:405-458.

Flemming, N. C. 1972. Eustatic and tectonic factors in the relative vertical displacement on the Aegean coast. In, The Mediterranean Sea: A natural sedimentation Laboratory. Edited by D. J. Stanley. Stroudsburg, Pennsylvania: Dowden, Hutchinson & Ross.

Fletcher, C. H., Van Pelt, J. E., Brush, G., and S., Sherman, J. 1993. Tidal wetland record of Holocene sea-level movements and climate history. Palaeogeography, Palaeoclimatology, Palaeoecology 102:177-213.

Friligos, N. 1985. Impact on Phytoplankton Populations of Sewage Discharges in the Saronikos Gulf (West Aegean). Water Research 19(9):1107-1118.

Gehrels, R. W. 1994. Determining the relative sea-level change from salt-marsh

foraminifera from the great marshes, Massachusetts: environmental controls. Palaeogeography, Palaeoclimatology, Palaeoecology 130:81-112.

Gehrels, R. W. and van de Plassche, O. 1999. The use of *Jadammina macrescens* (Brady) and *Balticammina pseudomacrescens* Brönnimann, Lutze and Whittaker (Protozoa: Foraminiferida) as sea-level indicators. Palaeogeography, Palaeoclimatology, Palaeoecology 149:89-101.

Goldstein, S. T. and Harben, E. B. 1993. Taphofacies implications of infaunal foraminiferal assemblages in a Georgia salt marsh, Sapelo Island. Micropaleontology 39:53-62.

Goldstein, S. T., Watkins, G. T., and Kuhn, R. M. 1995. Microhabitats of salt marsh foraminifera: St. Catherines Island, Georgia, USA. Marine Micropaleontology 26:17-29.

Goldstein, S. T. and Watkins, G. T. 1998. Elevation and the Distribution of Salt-marsh Foraminifera, St. Catherines Island, Georgia: A Taphonomic Approach. Palaios 13:570-580.

Guilbault, J. -P., Clague, J. J., and Lapointe, M.. 1995. Amount of subsidence during a late Holocene earthquake - evidence from fossil tidal marsh foraminifera at Vancouver Island, west coast of Canada. Palaeogeography, Palaeoclimatology, Palaeoecology 118:49-71.

Guilbault, J. -P. 1996. Foraminiferal Evidence for the amount of Coseismic Subsidence during a Late Holocene Earthquake on Vancouver Island, west coast of Canada. Quaternary Science Reviews 15:913-937.

Harrison, E. Z. and Bloom, A. L. 1977. Sedimentary Rates on tidal salt marshes in Connecticut. Journal of Sedimentary Petrology 47:1484-1490.

Hayward, B. W., and Hollis, C. J. 1994. Brackish foraminifera in New Zealand: a taxonomic and ecologic review. Micropaleontology 40(3):185-222.

Hayward, B. W., Grenfell, H. R., and Scott, D. B. 1999. Tidal range of marsh foraminifera for determining former sea-level heights in New Zealand. New Zealand Journalof Geology and Geophysics 42:395-413.

Heiri, O., Lotter, A. F., and Lemcke, G. 2000. Loss of ignition as a method for estimating organic and carbonate in sediments. Journal of Paleolimnology in press.

Hemphill-Haley, E. 1995. Diatom evidence for earthquake-induced subsidence and

tsunami 300 years ago in southern coastal Washington. Geological Society of America Bulletin 107:367-378.

Hippensteel, S. P. and Martin, R. E. 1999. Foraminifera as an indicator of overwash deposits, Barrier Island sediment supply, and Barrier Island evolution: Folly Island, South Carolina. Palaeogeography, Palaeoclimatology, Palaeoecology 149:115-125.

Hippensteel, S. P., Martin, R. E., Nikitina, D., and Pizzuto, J. E. 2000. The formation of holocene marsh foraminiferal assemblages, middle Atlantic coast, U.S.A.: implications for Holocene sea-level change. Journal of Foraminiferal Research 30(4):272-293.

Hopely, D. 1975. Contrasting evidence for Holocene sea levels with special reference to the Bowen-Whitsunday area of Queensland. In, Geographical Essays in honour of Gilbert J. Butland, edited by J. E. Hobbs and J. J. Pigram. Armidale: Department of Geography, University of New England.

Hopley, D. 1986. Beach rock as a sea-level indicator. In, Sea-level research: a manual for the collection and evaluation of data, edited by Orson van de Plassche. Norwich, England: Geo Books.

Horton, B. P. 1999. The distribution of contemporary intertidal foraminifera at Cowpen Marsh, Tees Estuary, UK: implications for studies of Holocene sea-level changes. Palaeogeography, Palaeoclimatology, Palaeoecology 149:127-149.

Isla, F. I. and Bujalesky, G. G. 2000. Cannibalisation of Holocene gravel beach-ridge plains, northern Tierra del Fuego, Argentina. Marine Geology 170:105-122.

Jackson, J. A., Gagnepain, J., Houseman, G., King, G. C. P., Papadimitriou, P., Soufleris, C., and Vireux, J. 1982. Seismicity, normal faulting, and the geomorphological Development of the Gulf of Corinth (Greece): the Corinth earthquakes of February and March, 1981. Earth Planetary Science Letters, 57:377-397.

Jackson, J. A. and White, N. J. 1989. Normal faulting in the upper continental crust: Observations from regions of active extension. Journal of Structural Geology 11:15-36.

Jennings, A. E., Nelson, A. R. 1992. Foraminiferal assemblage zones in Oregon tidal marshes--relation to marsh floral zones and sea level. Journal of Foraminiferal Research 22:13-29.

Jennings, A. E., Nelson, A., Scott, D. B., Aravena, J. C. 1995. Marsh foraminiferal assemblages in the Valdivia Estuary, South-central Chile, relative to vascular

plants and sea level. Journal of Coastal Research 11(1):107-123.

Jonasson, K. E. and Patterson, R. T. 1992. Preservation potential of marsh foraminifera from the Fraser River Delta, British Columbia. Micropaleontology 38:289-301.

Jones, G. D., and Ross, C. A. 1979. Seasonal distribution of foraminifera in Samish Bay Washington. Journal of Paleontology 53:245-257.

Kaye, C. A. and Barghoorn, E. S. 1964. Late Quaternary sea-level change and crustal rise at Boston, Massachusetts, with notes on the autocompaction of peat. Geological Society of America Bulletin 75:63-80.

Khalequzzaman, Md. 1989. Nature of sedimentary deposition in a salt marsh: Port Mahon, DE. M.S. Thesis, University of Delaware, Newark, 158 pp.

Laborel, J. and Laborel-Deguen, F. 1994. Biological indicators of relative sea-level variations and co-seismic displacements in the Mediterranean region. Journal of Coastal Research 10:395-415.

Lambeck, K. 1995. Late Pleistoncene and Holocene sea-level change in Greece and south-western Turkey: a separation of eustatic, isostatic and tectonic contributions. Geophysical Journal International 122:1022-1044.

Le Pichon, X. and Angelier, J. 1979. The Hellenic Arc and Trench System: a key to the Neotectonic Evolution of the eastern Mediterranean Area. Tectonophysics 60:1-42.

Lloyd, J. 2000. Combined foraminiferal and thecamoebian environmental reconstruction from an isolation basin in NW Scotland: implications for sea-level studies. Journal of Foraminiferal Research 30(4): 294-305.

Long, A. J. and Shennan, I. 1994. Sea-level changes in Washington and Oregon and the 'Earthquake Deformation Cycle'. Journal of Coastal Research 10:825-838.

Mariolakos, I. and Stiros, S. C. 1987. Quaternary deformation of the Isthmus and Gulf of Corinthos (Greece). Geology 15:225-228.

Martin, R. E. 1999. Taphonomy and temporal resolution of foraminiferal assemblages. In Modern Foraminifera, edited by Barun K. Sen Gupta. London: Kluwer Academic Publishers.

Mathewes, R. W. and Clague, J. J. 1994. Detection of large prehistoric earthquakes in the Pacific northwest by microfossil analysis. Science 264:688-691.

Murray, J. W. 1971. An Atlas of Recent British Foraminiferids. London: Heinemann.

Murray, J. W. 1991. Ecology and Palaeoecology of benthic foraminifera. Harlow, UK: Longman.

Murray, J. W. 2000. The enigma of the continued use of total assemblages in ecological studies of benthic foraminifera. Journal of Foraminiferal Research 30(3):244-245.

Nelson, A. R., Jennings, A. E., and Kashima, K. 1996. An earthquake history derived from stratigraphic and microfossil evidence of relative sea-level change at Coos Bay, southern coastal Oregon. GSA Bulletin 108(2):141-154.

Noller, J. S., Wells, L. E., Reinhardt, E., Rothaus, R. M. 1997. Subsidence of the Harbor at Kenchreai, Saronic Gulf, Greece, during the earthquakes of AD 400 and AD 1928. EOS (American Geophysical Union Transactions), 78:636.

Orson, R. A., Simpson, R. L., and Good, R. E. 1990. Rates of sediment accumulation in A tidal freshwater marsh. Journal of Sedimentary Petrology 60:859-869.

Ozarko, D. L., Patterson, R. T., and Williams, H. F. L. 1997. Marsh foraminifera from Nanaimo, British Columbia (Canada): implications of infaunal habitat and taphonomic biasing. Journal of Foraminiferal Research 27(1):51-68.

Papageorgiou, S., Arnold, M., Laborel, J., and Stiros, S. C. 1993. Seismic uplift of the harbour of ancient Aiegeira, Central Greece. International Journal of the Nautical Archaeology Society 22:275-281.

Papanikolaou, D., Lykousis, V., Chronis, G., and Pavlakis, P. 1988. A comparative study of neotectonic basins across the Hellenic arc: the Messiniakos, Argolikos, Saronikos, and Southern Evoikos Gulfs. Basin Research 1:167-176.

Papazachos, C. B. and Kiratzi, A. A. 1996. A detailed study of the active crustal deformation in the Aegean and surrounding area. Tectonophysics 253:129-153.

Patterson, R. T. and Fishbein, E. 1989. Re-examination of the statistical methods to determine the number of point counts needed for micropaleontological quantitative research. Journal of Paleontology, 63:245-248.

Patterson, R. T., 1990. Intertidal benthic foraminiferal biofacies on the Fraser River Delta, British Columbia: Modern distribution and paleoecological importance. Micropaleontology 36(3):229-244.

Patterson, T. R., Guilbault, J. -P., and Clague, J. J. 1999. Taphonomy of tidal marsh

foraminifera: implications of surface sample thickness for high-resolution sea-level studies. Palaeogeography, Palaeclimatology, Palaeoecology 149:199-211.

Peltier, W. R. 1994. Ice age paleotopography. Science 265:195-201.

Phleger, F. B. and Ewing, G. C. 1962. Sedimentology and Oceanography of Coastal Lagoons in Baja California, Mexico. GSA Bulletin 73:145-182.

Pirazzoli, P. A., Thommeret, J. & Y., Laborel, J. and Montaggioni, L. F. 1982. Crustal Block movements from Holocene shorelines: Crete and Antikythira (Greece). Tectonophysics 86:27-43.

Pirazzoli, P. A. 1986. Marine Notches. In Sea-level research: a manual for the collection and evaluation of data, edited by Orson van de Plassche. Norwich, England: Geo Books.

Pirazzoli, P. A., Stiros, S. C., Arnold, M., Laborel, J., Laborel-Deguen, F. and Papageorgiou, S. 1994. Episodic uplift deduced from Holocene shorelines in the Perachora Peninsula, Corinth area, Greece. Tectonophysics 229:201-209.

Pirazzoli, P. A. 1996. Uplift of ancient Greek coastal sites: study methods and results. In, Archaeoseismology , edited by S. Stiros and R. E. Jones. Athens, Greece: Institute of Geology and Mineral Exploration: British School at Athens.

Reaves, C. M. 1986. Organic matter and metabolizability and calcium carbonate Dissolution in near-shore marine muds. Journal of Sedimentary Petrology 56:486-494.

Reinhardt, E. G., Easton, N. A., and Patterson, T. R. 1996. Foraminiferal evidence of late Holocene sea-level change and Amerindian site distribution at Montague Harbour, British Columbia. Géographie physique et Quaternaire 50(1):35-46.

Rothaus, R., and Reinhardt, E. G. 1999. Prehistoric and Ancient Harbors in the Korinthia (Greece): A geoarchaeological approach for determining maritime trade patterns. 1999 Season. Unpublished report.

Saffert, H. and Thomas, E. 1998. Living foraminifera and total populations in salt marsh peat cores: Kelsey Marsh (Clinton, CT) and the Great Marshes (Barnstable, MA). Marine Micropaleontology 33:175-202.

Salmon, J. B. 1984. Wealthy Corinth: a history of the city to 338 BC. New York: Oxford University Press.

Scott, D. B. and Medioli, F. S. 1978. Vertical zonations of marsh foraminifera as

accurate indicators of former sea-levels. Nature 272:528-531.

Scott, D. B, Piper, D. J. W., and Panagos, A. G. 1979. Recent salt marsh and intertidal Mudflat Foraminifera from the western coast of Greece. Rivista Italiana di Paleontologia e Stratigrafia 85(1):243-266.

Scott, D. B., and Medioli, F. S. 1980. Quantitative studies of marsh foraminiferal Distributions in Nova Scotia: implications for sea-level studies. Cushman Foundation for Foraminiferal Research, Special Publication 17. 58p.

Scott, D. B. and Medioli, F. S. 1986. Foraminifera as Sea-level Indicators. In Sea-level research: a manual for the collection and evaluation of data. Edited by Orson van de Plassche. Norwich: Geo Books, Regency House.

Scott, D. B., Schnack, E. J., Ferrero, L., Espinosa, M., Barbosa, C. F. 1990. Recent Marsh foraminifera from the east coast of South America: Comparison to the Northern hemisphere. In, Palaeoecology, Biostratigraphy, Palaeoceanography And taxonomy of Agglutinated Foraminifera. Edited by C. Hemleben, M. A. Kaminski, W. Kuhnt, and D. B. Scott. Kluwer, Dordrecht, NATO/ASI Ser. C, 327:717-737.

Scott, D. B., Suter, J. R., and Kosters, E. C. 1991. Marsh foraminifera and arcellaceans of the lower Mississippi delta: controls on spatial distribution. Micropaleontology 37(4):373-392.

Scott, D. B. and Hermelin, J. O. R. 1993. A device for precision splitting of micropaleontological samples in liquid suspension. Journal of Paleontology 67:151-154.

Scott, D. B., Hasegawa, S., Saito, T., Ito, K., and Collins, E. 1995. Marsh foraminiferal and vegetation distributions in Nemuro Bay wetland areas, eastern Hokkaido. Transactions and Proceedings of the Palaeontological Society of Japan, New Series 180:282-295.

Scott, D. B., Collins, E. S., Duggan, J., Asioli, A., Saito, T., and Hasegawa, S. 1996. Pacific Rim marsh foraminiferal distributions: implications for sea-level studies. Journal Coastal Research 12(4):850-861.

Scott, D. K. and Leckis, R. M. 1990. Foraminiferal zonation of Great Sippewissett Salt Marsh (Falmouth, Massachusetts). Journal of Foraminiferal Research 20(3): 248-266.

Schwartz, M. L. and Tziavos, C. 1975. Sedimentary provinces of the Saronic Gulf system. Nature 257:573-575.

Sivan, D., Wdowinski, S., Lambeck, K., Galili, E., and Raban, A. 2001. Holocene sea-Level changes along the Mediterranean coast of Israel, based on archaeological Observations and numerical models. Palaeogeography, Palaeoclimatology, Palaeoecology 167:101-117.

Smith, R. K. 1987. Fossilization potential in modern shallow-water benthic foraminiferal Assemblages. Journal of Foraminiferal Research 17(2):117-122.

Sorel, D. 2000. A Pleistocene and still-active detachment fault and the origin of the Corinth-Patras rift, Greece. Geology 28(1):83-86.

Soter, S. 1998. Holocene uplift and subsidence of the Helike Delta, Gulf of Corinth, Greece. In Coastal Tectonics, edited by Stewart, I. S., and Vita-Finzi, C. London: Geological Society, London, Special Publications, 146:41-56.

Stanley, D. J. and Hait, A. K. 2000. Deltas, radiocarbon dating, and measurements of sediment storage and subsidence. Geology 28(4):295-298.

Stewart, I. And Vita-Finzi, C. 1996. Coastal uplift on normal faults; the Eliki Fault, Greece. Geophysical Research Letters 23(14):1853-1856.

Stiros, S. C., Arnold, M., Pirazzoli, P. A., Laborel, J., Laborel, F., and Papageorgiou, S. 1992. Historical coseismic uplift on Euboea Island, Greece. Earth and Planetary Science Letters 108:109-117.

Stiros, S. C., Laborel, J., Laborel-Deguen, F., Papageorgiou, S., Evin, J., and Pirazzoli, P. A. 2000. Seismic coastal uplift in a region of subsidence: Holocene raised shorelines of Samos Island, Aegean Sea, Greece. Marine Geology 170:41-58.

Stuiver, M., Reimer, P. J., Bard, E., Beck, J. W., Burr, G. S., Hughen, K. A., Kromer, B., McCormac, G., van der Plicht, J., and Spurk, M.. 1998. INTCAL98 Radiocarbon Age Calibration, 24, 000-0 cal BP. Radiocarbon 40(3):1041-1083.

Tooley, M. J. and Shennan, Ian 1987. Sea-level changes. Oxford, UK; New York, USA: B. Blackwell.

Van Andel, T. H. and Shackleton, J. C. 1982. Late Paleolithic and Mesolithic coastlines of Greece and the Aegean. Journal of Field Archaeology 9:445-454.

Vita-Finzi, C. 1993. Evaluating late Quaternary uplift in Greece and Cyprus. Magmatic Processes and plate tectonics. Geological Society Special Publications 76:417-424.

Williams, H. F. L. 1994. Intertidal benthic foraminiferal biofacies on the central Gulf Coast of Texas - Modern distribution and application to sea-level reconstruction. Micropaleontology 40:169:183.

Williams, F. L. 1999. Foraminiferal distributions in tidal marshes bordering the strait of Juan de Fuca: implications for paleoseismicity studies. Journal of Foraminiferal Research 29(3):196-208.

Zangger, E. 1991. Prehistoric coastal environments in Greece: the vanished landscapes Of Dimini Bay and Lake Lerna. Journal of Field Archaeology 18:1-15.

Zangger, E. 1996. Prehistoric earthquakes and their consequences, as preserved in Holocene sediments from Volos and Argos, Greece. In Archaeoseismology, edited by S. Stiros and R. E. Jones. Athens, Greece: Institute of Geology and Mineral Exploration: British School at Athens.

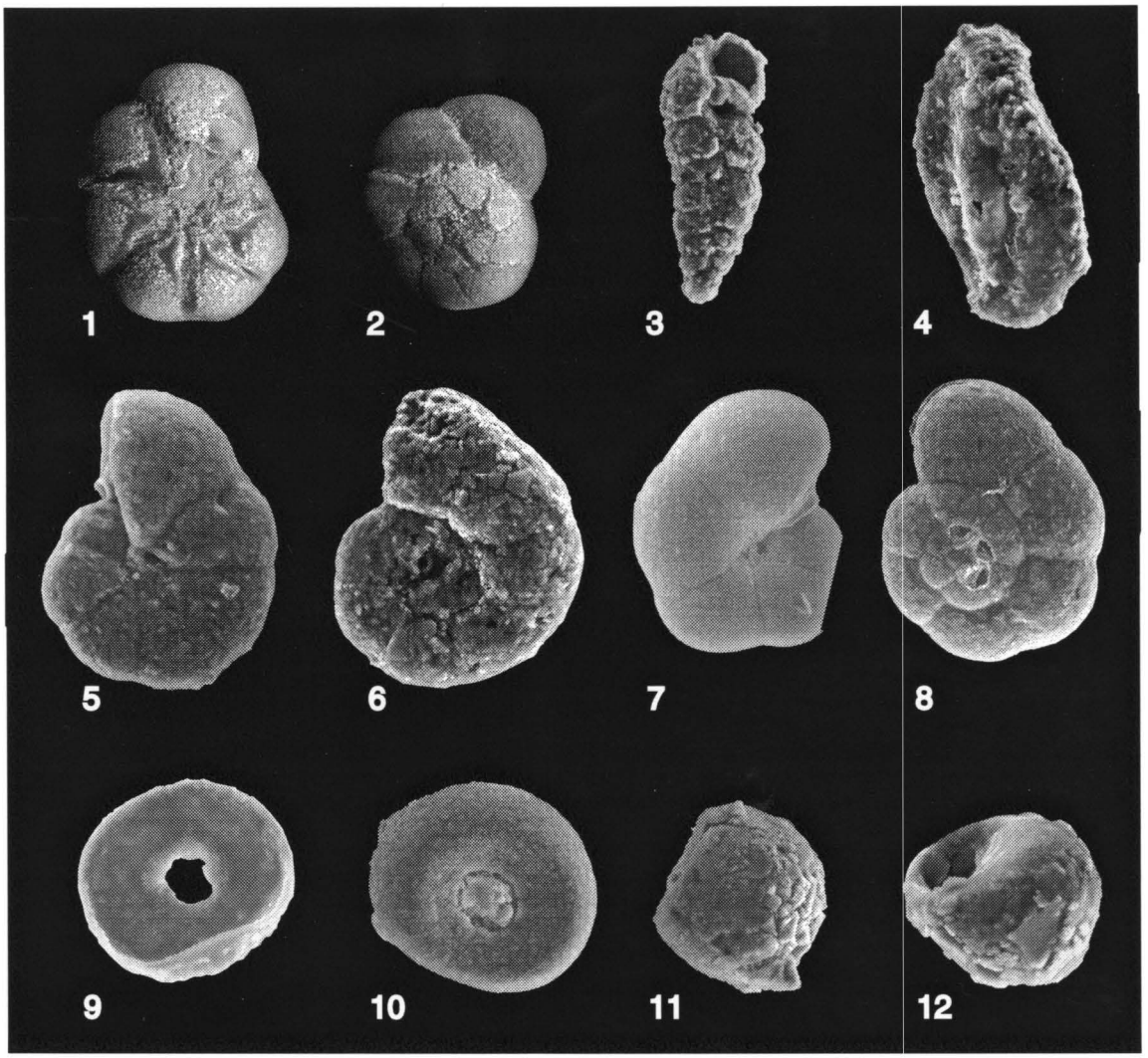

Plate 1

1, 2 *Ammonia beccarii tepida* (Cushman). 1 Ventral view, x295. 2, Dorsal view, x210. 3, *Textularia earlandi* (Parker). Side view, x465. 4, *Miliammina fusca* (Brady). View of fourchambered side, x500. 5, 6 *Trochammina macrescens* (Brady). 5, ventral view, x480. 6, dorsal view, x235. 7, 8 *Trochammina inflata* (Montagu). 7, ventral view, x235. 8, dorsal view, x205. 9, *Arcella vulgaris* (Ehrenberg). Top view, x750. 10, 11 *Centropyxis aculeata* (Ehrenberg). 10, side view, x800. 11, top view, x950. 12, *Centropyxis constricta* (Ehrenberg). Side view, x1100.

APPENDIX A: LIST OF IDENTIFIED FORAMINIFERA

All species reported in Appendix B are listed here although only the key species are illustrated (Plate 1). Species not illustrated in Plate 1 have references to published figures that portray their features.

Benthic Species

Suborder Textulariina

Miliammina fusca (Brady).
Textularia earlandi (Parker).
Trochammina inflata (Montagu).
Trochammina macrescens (Brady).

Suborder Rotaliina

Ammonia beccarii "tepida" (Cushman).
Discorinopsis aquayoi (Bermudez). Scott et al., 1979, pl.16, fig. 1, 2.

Arcellaceans

Arcella vulgaris (Ehrenberg).
Centropyxis aculeata (Ehrenberg).
Centropyxis constricta (Ehrenberg).
Difflugia oblonga (Ehrenberg). McCarthy et al., 1995, Fig. 2.

APPENDIX B: STANDARD ERROR AND 95% CONFIDENCE INTERVALS FOR CORE AND SURFACE MICROFAUNA

Ammonia beccarii "tepida" *Arcella vulgaris*

Sample	$X_i \pm 1.96\ SX_i$	Sample	$X_i \pm 1.96\ SX_i$	Sample	$X_i \pm 1.96\ SX_i$
C2(0.15m)	-	C3(-0.36m)	0.84 ± 0.04	C2(0.15m)	-
C2(0.07)	-	C3(-0.61m)	0.48 ± 0.16	C2(0.07)	-
C2(-0.07m)	-	C3(-0.83m)	0.54 ± 0.08	C2(-0.07m)	-
C2(-0.27m)	-	C3(-1.26m)	0.16 ± 0.10	C2(-0.27m)	-
C2(-0.31m)	-	C3(-1.80m)	0.20 ± 0.18	C2(-0.31m)	-
C2(-0.44m)	-	C3(-2.16m)	-	C2(-0.44m)	-
C2(-0.57m)	-	C3(-2.22m)	0.04 ± 0.04	C2(-0.57m)	-
C2(-0.74m)	-	C3(-2.33m)	-	C2(-0.74m)	-
C2(-1.11m)	-	C3(-2.82m)	0.22 ± 0.06	C2(-1.11m)	-
C1(0.29m)	-	S2(-0.29m)	-	C1(0.29m)	-
C1(-0.04m)	-	S3(-0.26m)	-	C1(-0.04m)	-
C1(-0.15m)	-	S4(-0.29m)	-	C1(-0.15m)	-
C1(-0.29m)	-	S5(-0.28m)	-	C1(-0.29m)	-
C1(-0.34m)	-	S6(-0.27m)	-	C1(-0.34m)	-
C1(-0.54m)	-	S7(-0.17m)	-	C1(-0.54m)	-
C1(-0.71m)	-	S8(-0.06m)	-	C1(-0.71m)	-
C1(-0.90m)	-	S9(-0.05m)	-	C1(-0.90m)	-
C1(-1.44m)	-	S10	-	C1(-1.44m)	-
C1(-1.65m)	-	S11	-	C1(-1.65m)	0.07 ± 0.06
C1(-1.84m)	-	S12(0.05m)	-	C1(-1.84m)	-
C1(-2.04m)	0.03 ± 0.04	S13(0.14m)	-	C1(-2.04m)	-
C1(-2.31m)	0.22 ± 0.22	S14(0.02m)	-	C1(-2.31m)	-
C1(-2.50m)	0.01 ± 0.02	S15(0.29m)	-	C1(-2.50m)	-
C1(-2.73m)	0.02 ± 0.04			C1(-2.73m)	-
C1(-2.82m)	0.05 ± 0.04			C1(-2.82m)	-
C1(-2.98m)	0.17 ± 0.16			C1(-2.98m)	-
C1(-3.12m)	0.49 ± 0.18			C1(-3.12m)	-
C1(-3.73m)	0.02 ± 0.04			C1(-3.73m)	-
C1(-3.98m)	0.37 ± 0.24			C1(-3.98m)	-
C1(-4.12m)	0.01 ± 0.02			C1(-4.12m)	-
C1(-4.43m)	-			C1(-4.43m)	-
C3(0.14m)	-			C3(0.14m)	-
C3(0.02m)	-			C3(0.02m)	-
C3(-0.09m)	-			C3(-0.09m)	-
C3(-0.22m)	0.93 ± 0.02			C3(-0.22m)	-

Arcella vulgaris *Centropyxis aculeata*

Sample	$X_i \pm 1.96\ SX_i$	Sample	$X_i \pm 1.96\ SX_i$	Sample	$X_i \pm 1.96\ SX_i$
C3(-0.36m)	-	C2(0.15m)	-	C3(-0.36m)	0.01 ± 0
C3(-0.61m)	-	C2(0.07)	0.28 ± 0.02	C3(-0.61m)	0.07 ± 0.08
C3(-0.83m)	-	C2(-0.07m)	0.99 ± 0.04	C3(-0.83m)	0.21 ± 0.08
C3(-1.26m)	-	C2(-0.27m)	-	C3(-1.26m)	0.58 ± 0.12
C3(-1.80m)	-	C2(-0.31m)	0.14 ± 0.02	C3(-1.80m)	0.8 ± 0.18
C3(-2.16m)	-	C2(-0.44m)	-	C3(-2.16m)	-
C3(-2.22m)	-	C2(-0.57m)	0.04 ± 0.02	C3(-2.22m)	0.93 ± 0.04
C3(-2.33m)	-	C2(-0.74m)	0.52 ± 0.08	C3(-2.33m)	1.0 ± 0
C3(-2.82m)	-	C2(-1.11m)	0.61 ± 0.08	C3(-2.82m)	0.68 ± 0.08
S2(-0.29m)	-	C1(0.29m)	0.05 ± 0.02	S2(-0.29m)	-
S3(-0.26m)	0.04 ± 0.02	C1(-0.04m)	0.54 ± 0.08	S3(-0.26m)	-
S4(-0.29m)	-	C1(-0.15m)	-	S4(-0.29m)	-
S5(-0.28m)	-	C1(-0.29m)	-	S5(-0.28m)	-
S6(-0.27m)	-	C1(-0.34m)	0.17 ± 0.06	S6(-0.27m)	-
S7(-0.17m)	-	C1(-0.54m)	0.19 ± 0.16	S7(-0.17m)	0.02 ± 0
S8(-0.06m)	0.02 ± 0.04	C1(-0.71m)	-	S8(-0.06m)	0.02 ± 0.02
S9(-0.05m)	-	C1(-0.90m)	-	S9(-0.05m)	-
S10	-	C1(-1.44m)	-	S10	-
S11	-	C1(-1.65m)	0.93 ± 0.06	S11	0.09 ± 0.02
S12(0.05m)	-	C1(-1.84m)	0.89 ± 0.12	S12(0.05m)	-
S13(0.14m)	0.03 ± 0.02	C1(-2.04m)	0.93 ± 0.06	S13(0.14m)	0.11 ± 0.02
S14(0.02m)		C1(-2.31m)	0.74 ± 0.24	S14(0.02m)	0.71 ± 0.2
S15(0.29m)		C1(-2.50m)	0.94 ± 0.04	S15(0.29m)	0.83 ± 0.06
		C1(-2.73m)	0.95 ± 0.06		
		C1(-2.82m)	0.87 ± 0.06		
		C1(-2.98m)	0.43 ± 0.2		
		C1(-3.12m)	0.45 ± 0.18		
		C1(-3.73m)	0.96 ± 0.06		
		C1(-3.98m)	0.63 ± 0.24		
		C1(-4.12m)	0.95 ± 0.04		
		C1(-4.43m)	0.94 ± 0.06		
		C3(0.14m)	0.29 ± 0.04		
		C3(0.02m)	-		
		C3(-0.09m)	0.05 ± 0.02		
		C3(-0.22m)	0.01 ± 0		

Centropyxis constricta *Discorinopsis aquayoi*

Sample	$X_i \pm 1.96\ SX_i$	Sample	$X_i \pm 1.96\ SX_i$	Sample	$X_i \pm 1.96\ SX_i$
C2(0.15m)	-	C3(-0.36m)	-	C2(0.15m)	-
C2(0.07)	0.06 ± 0	C3(-0.61m)	-	C2(0.07)	-
C2(-0.07m)	0.01 ± 0.04	C3(-0.83m)	-	C2(-0.07m)	-
C2(-0.27m)	-	C3(-1.26m)	-	C2(-0.27m)	-
C2(-0.31m)	-	C3(-1.80m)	-	C2(-0.31m)	-
C2(-0.44m)	-	C3(-2.16m)	-	C2(-0.44m)	-
C2(-0.57m)	-	C3(-2.22m)	0.03 ± 0.02	C2(-0.57m)	-
C2(-0.74m)	0.17 ± 0.06	C3(-2.33m)	-	C2(-0.74m)	-
C2(-1.11m)	0.07 ± 0.04	C3(-2.82m)	0.07 ± 0.04	C2(-1.11m)	-
C1(0.29m)	0.02 ± 0.02	S2(-0.29m)	-	C1(0.29m)	-
C1(-0.04m)	-	S3(-0.26m)	0.02 ± 0.02	C1(-0.04m)	-
C1(-0.15m)	-	S4(-0.29m)	0.04 ± 0	C1(-0.15m)	-
C1(-0.29m)	-	S5(-0.28m)	-	C1(-0.29m)	-
C1(-0.34m)	-	S6(-0.27m)	-	C1(-0.34m)	-
C1(-0.54m)	0.19 ± 0.16	S7(-0.17m)	-	C1(-0.54m)	-
C1(-0.71m)	-	S8(-0.06m)	0.18 ± 0.04	C1(-0.71m)	-
C1(-0.90m)	-	S9(-0.05m)	-	C1(-0.90m)	-
C1(-1.44m)	-	S10	-	C1(-1.44m)	-
C1(-1.65m)	-	S11	-	C1(-1.65m)	-
C1(-1.84m)	-	S12(0.05m)	-	C1(-1.84m)	-
C1(-2.04m)	0.03 ± 0.04	S13(0.14m)	0.01 ± 0.02	C1(-2.04m)	-
C1(-2.31m)	0.02 ± 0.08	S14(0.02m)	-	C1(-2.31m)	-
C1(-2.50m)	0.04 ± 0.02	S15(0.29m)	0.15 ± 0.06	C1(-2.50m)	-
C1(-2.73m)	0.04 ± 0.04			C1(-2.73m)	-
C1(-2.82m)	0.07 ± 0.04			C1(-2.82m)	-
C1(-2.98m)	-			C1(-2.98m)	-
C1(-3.12m)	-			C1(-3.12m)	-
C1(-3.73m)	0.02 ± 0.04			C1(-3.73m)	-
C1(-3.98m)	-			C1(-3.98m)	-
C1(-4.12m)	0.04 ± 0.04			C1(-4.12m)	-
C1(-4.43m)	0.04 ± 0.04			C1(-4.43m)	0.01 ± 0.02
C3(0.14m)	0.03 ± 0.02			C3(0.14m)	-
C3(0.02m)	-			C3(0.02m)	-
C3(-0.09m)	-			C3(-0.09m)	-
C3(-0.22m)	-			C3(-0.22m)	-

Discorinopsis aquayoi *Miliammina fusca*

Sample	$X_i \pm 1.96\ SX_i$	Sample	$X_i \pm 1.96\ SX_i$	Sample	$X_i \pm 1.96\ SX_i$
C3(-0.36m)	0.01 ± 0	C2(0.15m)	0.01 ± 0	C3(-0.36m)	-
C3(-0.61m)	-	C2(0.07)	-	C3(-0.61m)	-
C3(-0.83m)	-	C2(-0.07m)	-	C3(-0.83m)	0.02 ± 0.02
C3(-1.26m)	-	C2(-0.27m)	0.01 ± 0	C3(-1.26m)	-
C3(-1.80m)	-	C2(-0.31m)	-	C3(-1.80m)	-
C3(-2.16m)	-	C2(-0.44m)	-	C3(-2.16m)	-
C3(-2.22m)	-	C2(-0.57m)	-	C3(-2.22m)	-
C3(-2.33m)	-	C2(-0.74m)	-	C3(-2.33m)	-
C3(-2.82m)	-	C2(-1.11m)	0.01 ± 0.02	C3(-2.82m)	-
S2(-0.29m)	0.01 ± 0	C1(0.29m)	0.05 ± 0.02	S2(-0.29m)	0.03 ± 0.02
S3(-0.26m)	0.01 ± 0	C1(-0.04m)	-	S3(-0.26m)	0.38 ± 0.04
S4(-0.29m)	-	C1(-0.15m)	-	S4(-0.29m)	0.23 ± 0.02
S5(-0.28m)	-	C1(-0.29m)	-	S5(-0.28m)	0.08 ± 0
S6(-0.27m)	-	C1(-0.34m)	0.01 ± 0.02	S6(-0.27m)	0.03 ± 0.02
S7(-0.17m)	-	C1(-0.54m)	0.19 ± 0.16	S7(-0.17m)	0.1 ± 0.02
S8(-0.06m)	0.02 ± 0.02	C1(-0.71m)	-	S8(-0.06m)	0.49 ± 0.06
S9(-0.05m)	-	C1(-0.90m)	-	S9(-0.05m)	0.58 ± 0.22
S10	-	C1(-1.44m)	-	S10	0.5 ± 0.27
S11	0.06 ± 0.02	C1(-1.65m)	-	S11	0.11 ± 0.02
S12(0.05m)	-	C1(-1.84m)	-	S12(0.05m)	0.04 ± 0.02
S13(0.14m)	0.02 ± 0.02	C1(-2.04m)	-	S13(0.14m)	0.8 ± 0.04
S14(0.02m)	0.16 ± 0.16	C1(-2.31m)	-	S14(0.02m)	-
S15(0.29m)	-	C1(-2.50m)	-	S15(0.29m)	-
		C1(-2.73m)	-		
		C1(-2.82m)	-		
		C1(-2.98m)	-		
		C1(-3.12m)	-		
		C1(-3.73m)	-		
		C1(-3.98m)	-		
		C1(-4.12m)	-		
		C1(-4.43m)	-		
		C3(0.14m)	0.02 ± 0		
		C3(0.02m)	0.04 ± 0.02		
		C3(-0.09m)	-		
		C3(-0.22m)	-		

Textularia earlandi *Trochammina inflata*

Sample	$X_i \pm 1.96\ SX_i$	Sample	$X_i \pm 1.96\ SX_i$	Sample	$X_i \pm 1.96\ SX_i$
C2(0.15m)	-	C3(-0.36m)	-	C2(0.15m)	0.44 ± 0.02
C2(0.07)	-	C3(-0.61m)	0.02 ± 0.04	C2(0.07)	0.11 ± 0
C2(-0.07m)	-	C3(-0.83m)	-	C2(-0.07m)	-
C2(-0.27m)	-	C3(-1.26m)	-	C2(-0.27m)	0.68 ± 0.02
C2(-0.31m)	-	C3(-1.80m)	-	C2(-0.31m)	0.38 ± 0.02
C2(-0.44m)	-	C3(-2.16m)	-	C2(-0.44m)	0.43 ± 0.02
C2(-0.57m)	-	C3(-2.22m)	-	C2(-0.57m)	0.4 ± 0.02
C2(-0.74m)	-	C3(-2.33m)	-	C2(-0.74m)	0.09 ± 0.04
C2(-1.11m)	-	C3(-2.82m)	-	C2(-1.11m)	0.01 ± 0.02
C1(0.29m)	-	S2(-0.29m)	-	C1(0.29m)	0.45 ± 0.04
C1(-0.04m)	-	S3(-0.26m)	-	C1(-0.04m)	0.23 ± 0.06
C1(-0.15m)	-	S4(-0.29m)	-	C1(-0.15m)	0.47 ± 0.02
C1(-0.29m)	-	S5(-0.28m)	-	C1(-0.29m)	0.73 ± 0.02
C1(-0.34m)	-	S6(-0.27m)	-	C1(-0.34m)	0.58 ± 0.08
C1(-0.54m)	-	S7(-0.17m)	-	C1(-0.54m)	0.42 ± 0.2
C1(-0.71m)	-	S8(-0.06m)	-	C1(-0.71m)	0.04 ± 0.02
C1(-0.90m)	-	S9(-0.05m)	-	C1(-0.90m)	0.51 ± 0.04
C1(-1.44m)	-	S10	-	C1(-1.44m)	-
C1(-1.65m)	-	S11	-	C1(-1.65m)	-
C1(-1.84m)	-	S12(0.05m)	-	C1(-1.84m)	0.11 ± 0.12
C1(-2.04m)	-	S13(0.14m)	-	C1(-2.04m)	-
C1(-2.31m)	-	S14(0.02m)	-	C1(-2.31m)	-
C1(-2.50m)	-	S15(0.29m)	-	C1(-2.50m)	0.01 ± 0.02
C1(-2.73m)	-			C1(-2.73m)	-
C1(-2.82m)	-			C1(-2.82m)	0.01 ± 0.02
C1(-2.98m)	-			C1(-2.98m)	-
C1(-3.12m)	-			C1(-3.12m)	0.04 ± 0.06
C1(-3.73m)	-			C1(-3.73m)	-
C1(-3.98m)	-			C1(-3.98m)	-
C1(-4.12m)	-			C1(-4.12m)	-
C1(-4.43m)	-			C1(-4.43m)	0.01 ± 0.02
C3(0.14m)	0.08 ± 0.02			C3(0.14m)	0.55 ± 0.04
C3(0.02m)	-			C3(0.02m)	0.59 ± 0.04
C3(-0.09m)	-			C3(-0.09m)	0.59 ± 0.02
C3(-0.22m)	-			C3(-0.22m)	0.03 ± 0.02

Trochammina inflata *Trochammina macrescens*

Sample	$X_i \pm 1.96\ SX_i$	Sample	$X_i \pm 1.96\ SX_i$	Sample	$X_i \pm 1.96\ SX_i$
C3(-0.36m)	0.1 ± 0.02	C2(0.15m)	0.54 ± 0.02	C3(-0.36m)	-
C3(-0.61m)	0.28 ± 0.14	C2(0.07)	0.56 ± 0.02	C3(-0.61m)	-
C3(-0.83m)	0.22 ± 0.08	C2(-0.07m)	-	C3(-0.83m)	0.02 ± 0.02
C3(-1.26m)	0.16 ± 0.1	C2(-0.27m)	0.31 ± 0.02	C3(-1.26m)	-
C3(-1.80m)	-	C2(-0.31m)	0.49 ± 0.04	C3(-1.80m)	-
C3(-2.16m)	-	C2(-0.44m)	0.54 ± 0.02	C3(-2.16m)	-
C3(-2.22m)	-	C2(-0.57m)	0.56 ± 0.02	C3(-2.22m)	-
C3(-2.33m)	-	C2(-0.74m)	0.22 ± 0.06	C3(-2.33m)	-
C3(-2.82m)	-	C2(-1.11m)	0.31 ± 0.08	C3(-2.82m)	0.03 ± 0.02
S2(-0.29m)	0.67 ± 0.06	C1(0.29m)	0.43 ± 0.04	S2(-0.29m)	0.29 ± 0.06
S3(-0.26m)	0.48 ± 0.04	C1(-0.04m)	0.24 ± 0.06	S3(-0.26m)	0.07 ± 0.02
S4(-0.29m)	0.51 ± 0.02	C1(-0.15m)	0.53 ± 0.02	S4(-0.29m)	0.21 ± 0.02
S5(-0.28m)	0.49 ± 0.02	C1(-0.29m)	0.27 ±	S5(-0.28m)	0.43 ± 0.02
S6(-0.27m)	0.64 ± 0.02	C1(-0.34m)	0.01 ± 0.02	S6(-0.27m)	0.32 ± 0.02
S7(-0.17m)	0.52 ± 0.02	C1(-0.54m)	0.19 ± 0.16	S7(-0.17m)	0.35 ± 0.02
S8(-0.06m)	0.15 ± 0.04	C1(-0.71m)	-	S8(-0.06m)	0.06 ± 0.02
S9(-0.05m)	0.04 ± 0.1	C1(-0.90m)	-	S9(-0.05m)	0.38 ± 0.22
S10	0.1 ± 0.18	C1(-1.44m)	-	S10	0.4 ± 0.27
S11	0.37 ± 0.04	C1(-1.65m)	-	S11	0.37 ± 0.04
S12(0.05m)	0.51 ± 0.04	C1(-1.84m)	-	S12(0.05m)	0.44 ± 0.04
S13(0.14m)	-	C1(-2.04m)	-	S13(0.14m)	0.03 ± 0.02
S14(0.02m)	-	C1(-2.31m)	-	S14(0.02m)	0.13 ± 0.14
S15(0.29m)	-	C1(-2.50m)	-	S15(0.29m)	0.01 ± 0.02
		C1(-2.73m)	-		
		C1(-2.82m)	-		
		C1(-2.98m)	-		
		C1(-3.12m)	-		
		C1(-3.73m)	-		
		C1(-3.98m)	-		
		C1(-4.12m)	-		
		C1(-4.43m)	-		
		C3(0.14m)	0.02 ± 0		
		C3(0.02m)	0.04 ± 0.02		
		C3(-0.09m)	-		
		C3(-0.22m)	-		

APPENDIX C: GRAIN SIZE STATISTICS FOR KORPHOS CORE SEDIMENTS

Fine-Silt Lithofacies			
Sample	**Mean**	**Standard Deviation (1σ)**	**Skew**
C1(-0.04)	11.18	13.96	1.67
C1(-0.29)	23.76	46.32	3.13
C1(-0.90)	5.309	6.64	2.63
C2(0.15)	8.678	9.446	1.65
C3(-0.36)	10.01	11.85	1.69
Mean	11.78	17.64	
Standard Deviation	7.04	16.26	
Medium/Coarse-Silt Lithofacies			
Sample	**Mean**	**Standard Deviation (1σ)**	**Skew**
C1(-3.21m)	50.87	62.4	1.15
C3(-0.83m)	54.56	67.79	1.1
C3(-1.8m)	46	56.45	1.26
C3(-2.54m)	30.29	34.78	1.02
Mean	45.43	55.36	
Standard Deviation (1σ)	10.7	14.5	
Coarse-Silt Lithofacies			
Sample	**Mean**	**Standard Deviation (1σ)**	**Skew**
C1(0.29m)	26.84	26.2	0.97
C1(-0.15m)	66.77	62.45	0.49
C1(-0.34m)	42.5	60.06	1.47
C1(-0.71m)	54.33	56.58	0.79
C1(-1.65m)	81.58	70.23	0.28
C1(-1.96m)	75.94	73.96	0.55
C1(-2.52m)	64.4	62.28	0.46
C1(-2.84m)	58.1	62.6	0.74
C2(0.07m)	59.68	79.96	1.29
C2(-0.07m)	79.74	68.95	0.34
C2(-0.27m)	43.24	63.71	1.57
C2(-0.31m)	57.46	61.47	0.85
C2(-0.44m)	73.9	70.98	0.46
C2(-0.57m)	51.58	63.49	1.27
C2(-0.74m)	43.72	59	1.34
C2(-1.11m)	16.53	24.43	2.11
C3(-0.09m)	73.83	61.79	0.13
C3(-0.22m)	73.75	75.26	0.54
C3(-1.26m)	69.58	79.89	0.88
C3(-2.31m)	71.46	69.62	0.64
Mean	59.25	62.65	
Standard Deviation (1σ)	17.64	14.42	

Very Fine-Sand Lithofacies			
Sample	**Mean**	**Standard Deviation (1σ)**	**Skew**
C1(-1.84m)	70.28	63.94	0.30
C1(-2.1m)	87.22	74.42	0.22
C1(-2.32m)	71.82	55.76	-0.06
C1(-2.37m)	56.16	55.02	0.47
C1(-2.45m)	120.8	85.36	0.28
C1(-3.05m)	60.01	58.9	0.45
C3(0.02m)	93.51	66.38	0.063
C3(0.61m)	81.05	67.93	0.2
Mean	80.11	65.96	
Standard Deviation (1σ)	20.80	10.21	
Fine-Sand Lithofacies			
Sample	**Mean**	**Standard Deviation (1σ)**	**Skew**
C1(-0.54m)	169.5	152.1	0.85
C1(-2.5m)	172.8	134.3	0.93
C1(-3.98m)	141.4	161.2	1.96
C3(0.14m)	146.7	161.2	0.95
C3(-2.22m)	198.9	174.2	0.56
Mean	165.86	156.6	
Standard Deviation (1σ)	23.01	14.74	